

# **For Reference**


---

**NOT TO BE TAKEN FROM THIS ROOM**



Ex LIBRIS  
UNIVERSITATIS  
ALBERTAENSIS





Digitized by the Internet Archive  
in 2023 with funding from  
University of Alberta Library

<https://archive.org/details/Hibbs1972>







THE UNIVERSITY OF ALBERTA

A STUDY OF APERIODIC, SPATIALLY TIME VARYING TWO-  
DIMENSIONAL SOURCES IN ELECTROMAGNETIC INDUCTION

by



ROY DEAN HIBBS, JR.

A THESIS

SUBMITTED TO THE FACULTY OF GRADUATE STUDIES AND RESEARCH

IN

PARTIAL FULFILLMENT OF THE REQUIREMENTS FOR THE DEGREE OF

MASTER OF SCIENCE

Department of Physics

Edmonton, Alberta

Fall, 1972.







UNIVERSITY OF ALBERTA

FACULTY OF GRADUATE STUDIES AND RESEARCH

The undersigned certify that they have read, and recommend to the Faculty of Graduate Studies and Research for acceptance, a thesis entitled A STUDY OF APERIODIC, SPATIALLY TIME VARYING TWO-DIMENSIONAL SOURCES IN ELECTROMAGNETIC INDUCTION, submitted by Roy Dean Hibbs, Jr. in partial fulfillment of the requirements for the degree of Master of Science.



## ABSTRACT

Electromagnetic induction in the earth by a generalized two-dimensional source is considered. The global and local problems are discussed in detail. A description of the two-dimensional E and H polarization cases is presented along with a review of the determinacy and the various methods used to solve the problem.

A comprehensive discussion of the source is given and solutions for selected non-uniform sources are described.

The electromagnetic induction by a symmetric ionospheric current distribution which is sinusoidally time dependent over a horizontally stratified earth is investigated and a method is presented for the calculation of perturbations of such fields by embedded inhomogeneities. This method is then extended to non-symmetric current distributions over layered and laterally inhomogeneous subsurfaces.

An aperiodic source is obtained by summing the single frequency solutions for layered subsurfaces in a Fourier transformation. By superposition of the electromagnetic fields of separate aperiodic, non-uniform current sources which vary independently with time a source which exhibits spatial variation with time is





obtained.





## ACKNOWLEDGEMENTS

The author wishes to express his sincere thanks to Dr. F. W. Jones for his supervision and invaluable assistance in this research. The author also wishes to express his appreciation to Dr. G. Rostoker and Dr. J. Jacobs for their encouragement and support.



## TABLE OF CONTENTS

	Page
1. INTRODUCTION .....	1
1.1 General .....	1
1.2 Global and Local Problems .....	2
1.2.a Global Problems .....	3
1.2.b Local Problems .....	6
1.3 The Two-Dimensional Problem .....	10
1.3.a E and H Polarizations .....	10
1.3.b Determinacy of the Two-Dimensional Problem .....	12
1.4 Methods for Solving the Two-Dimensional Problem .....	18
2. SOURCE DISCUSSION .....	23
3. SOLUTIONS FOR NON-UNIFORM SOURCES .....	29
3.1 Two-Dimensional Solutions for Non- Uniform Sources over Layered Media .....	29
3.1.a Line Current Source .....	29
3.1.b Gaussian Current Source .....	33
3.2. Two-Dimensional Solutions for Non- Uniform Sources over Laterally Inhomogeneous	





Media .....	37
3.2.a Iterative Solutions .....	38
3.2.b Combined Solutions for Non-Uniform Source and Laterally Non-Uniform Subsurface .....	46

4. AN INVESTIGATION OF THE SOURCE EFFECTS IN SYMMETRIC AND NON-SYMMETRIC IONOSPHERIC CURRENT DISTRIBUTIONS .....	49
4.1 The Symmetric Current Source Distribution .....	49
4.1.a Mathematical Formulation of the Boundary Conditions .....	49
4.1.b Variation of $ E_x $ , $ H_y $ and $ H_z $ due to a Non-Uniform Source above a Layered Conductor .....	51
4.1.c The Solution for a Laterally Inhomogeneous Structure and Apparent Resistivity Curves. ....	54
4.2 The Non-Symmetric Current Source Distribution .....	56
4.2.a Mathematical Formulation of the Boundary Conditions .....	56
4.2.b Variation of $ E_x $ , $ H_y $ and $ H_z $ due to a Non-Symmetric Source and Apparent	





Resistivity Curves. ....	63
4.2.c The Solution for a Laterally Inhomogeneous Structure and Apparent Resistivity Curves. ....	65
5. ELECTROMAGNETIC INDUCTION IN THE EARTH BY AN APERIODIC NON-UNIFORM CURRENT SOURCE .....	68
5.1.a The Two-Dimensional Double Current System .....	68
5.1.b Method of Solution .....	70
5.1.c The Two-Dimensional Aperiodic Spatially Varying Double Current Solution. .....	75
6. RECOMMENDATIONS FOR FURTHER RESEARCH .....	78
REFERENCES .....	79



## LIST OF FIGURES

	Page
Fig. 1.1 Coordinate System. ....	10a
Fig. 3.1 Coordinate System. ....	29a
Fig. 3.2 The General Two-Dimensional Model. ....	39a
Fig. 3.3 Grid Point Diagram. ....	40a
Fig. 4.1 Coordinate System (Gaussian Source). ....	49a
Fig. 4.2 $ H_z $ , $ H_y $ and $ E_x $ Profiles with Height (Gaussian Source). ....	52a
Fig. 4.3 E-field Profiles for Varying Source Width. ....	54a
Fig. 4.4 Conductivity Configuration. ....	55a
Fig. 4.5 Source Location. ....	55b
Fig. 4.6 Apparent Resistivity Curves (Gaussian Source). .....	55c



Fig. 4.7 Apparent Resistivity Curves for Different Positions over the Lateral Inhomogeneity (Gaussian Source). . . . .55d

Fig. 4.8 The Coordinate System (Non-Symmetric Source). . . . .56a

Fig. 4.9  $|H_z|$ ,  $|H_y|$  and  $|E_x|$  Profiles with Height (Non-Symmetric Source). . . . .63a

Fig. 4.10 Apparent Resistivity Curves (Non-Symmetric Source). . . . .65a

Fig. 4.11 Conductivity Configuration. . . . .65b

Fig. 4.12 Source Location. . . . .65c

Fig. 4.13 Apparent Resistivity Curves (Non-Symmetric Source). . . . .66a

Fig. 4.14 Apparent Resistivity Curves for Different Positions over the Lateral Inhomogeneity (Non-Symmetric Source). . . . .66b





Fig. 5.1 Coordinate System. ....70a

Fig. 5.2 Source Position. ....70b

Fig. 5.3 Time Variation of the Current Sources. ....74a

Fig. 5.4 Variation of  $H_y$  and  $H_z$  with Time (Symmetric Source). ....75a

Fig. 5.5 Variation of  $H_y$  and  $H_z$  with Time (Non-Symmetric Source). ....75b

Fig. 5.6 Variation of  $H_y$  and  $H_z$  with Time for the Superimposed Symmetric and Non-Symmetric Sources. ....75c

Fig. 5.7 Spatial Profiles of  $H_y$  and  $H_z$  with Time. ...76a

Fig. 5.8 Spatial Profiles of  $H_y$  and  $H_z$  with Time. ...76b

Fig. 5.9 Spatial Profiles of  $H_y$  and  $H_z$  with Time. ...76c



## 1. INTRODUCTION

### 1.1 General

The inductive response of the electrically conducting earth's interior to external geomagnetic variations can be inferred from the observed surface fields. Currents induced in the earth by external oscillating electromagnetic fields considerably modify the surface field values. These external sources consist of current systems of finite extent flowing in the ionosphere or above. In general the geomagnetic variations produced by these current systems are transient in time.

In this thesis the global and local problems in electromagnetic induction are discussed and the general two-dimensional local perturbation problem is considered together with various methods for its solution. The source effects due to non-uniform source current distributions are then investigated and solutions for selected non-uniform sources over a layered earth are presented. A method for solution over a laterally non-uniform earth is described. Symmetric and non-symmetric ionospheric current distributions are considered and solutions for such current distributions which vary sinusoidally with time over a uniformly layered earth as well as over a laterally inhomogeneous earth are computed





and compared with uniform source results. The mathematical formulation of the boundary conditions necessary to obtain these solutions is given. Aperiodic sources are investigated by the summation of the solutions for different frequencies through the use of the Fourier transform. By the superposition of solutions for different current distributions which do not vary sinusoidally in time, a source which changes spatially with time can be obtained. The magnetic field components of such a source over a layered earth of finite conductivity are then computed and profiles of the components obtained.

## 1.2 Global and Local Problems

The mathematical problems encountered in the study of earth currents are of two types. The first type involves inducing fields of global dimensions with averaged conductivities for the earth as a whole; these are known as global problems. The second type may or may not involve inducing fields of global dimensions but the conductivity values are definitely local values; these are known as local problems. Following the discussion by Price (1964) these problems are further considered.



### 1.2.a Global Problems

In the first group of problems, since we are interested in large regions having dimensions comparable to those of the earth, it is necessary to use spherical polar coordinates. The electrical conductivity  $v$  is then treated as a smoothed function of the coordinates  $(r, \theta, \phi)$  at any point within the earth. This function will not take into account any local variations in conductivity (which may be considerable) but only large scale variations of suitably defined average  $v$  for any region. For this problem the currents induced in any earth model will depend on the nature and distribution of the inducing field. The first step in solving such a problem is to express the inducing field in terms of spherical harmonics (assumed given). The induction effect of each harmonic is then studied separately and the result obtained from the summation of all the harmonics. The basic theory and method of solution for this type of problem is straightforward, though the calculation may be difficult and laborious.

One global problem which has been extensively studied is that of the induction, by a varying magnetic field, of electric currents in a spherical conductor in which the conductivity is a function of  $r$ , the distance



from the center of the earth. Lamb (1883) treated the case where  $v$  is uniform, and Lamb's solution was used by Schuster (1889) in his discussion of the internal and external parts of the magnetic daily variations. Chapman (1919) and Chapman and Whitehead (1922) made further applications of Lamb's solution. Price (1930, 1931) extended Lamb's solution to aperiodic fields and Chapman and Price (1930) then used this extension to discuss the induced part of the field of magnetic storms. The more general case when  $v$  is any function of  $r$  was studied by Lahiri and Price (1939). They developed both formulae and methods of calculation for both periodic and aperiodic fields when dealing with any distribution of conductivity within the sphere  $r=a$  that can be expressed in the form:

$$v=v^0 (qa/r)^m \text{ for } r<qa<a \text{ and } v=0 \text{ for } r>qa \quad (1.1)$$

where  $v^0$ ,  $q$  and  $m$  are constants.

Lahiri and Price (1939) applied their results to investigate the earth's conductivity to considerable depths and many applications of their formulae and methods have since been made by other investigators (e.g. Rikitake, 1950).





Apparently there have been no successful attempts to obtain solutions (analytical or numerical) for the induction of currents in a spherical conductor, when the conductivity is not only a function of  $r$  but also depends upon  $\theta$  or  $\phi$  or both. It seems reasonable that, except within the outermost 700 km. of the earth, the variation of the conductivity with  $r$  is far more important than any dependence upon  $\theta$  or  $\phi$ .

The variation of  $v$  with  $\theta$  and  $\phi$  within the crust is of importance in both global and local problems. For example, the conductivity of the oceans is several orders of magnitude greater than that of the continents. Non-uniform spherical shells are useful in modeling the global effects of currents induced in the crust. Price (1949) has given the basic theory of electromagnetic induction in non-uniform thin sheets and shells and applications have been made by Ashour (1950), Rikitake (1960), and others.

For very slowly varying magnetic fields it is not possible to treat the crust as a thin shell by itself, because of the mutual induction between the crust and conducting mantle below. This point was illustrated by Rikitake (1961) in his discussion of the currents induced in the oceans by daily variations.



### 1.2.b Local Problems

In the local problems the sphericity of the earth is ignored, and the earth is treated as a semi-infinite plane body having a non-uniform distribution of conductivity, where our attention is confined to some limited portion of the conductor. However, the inducing field is usually of large dimensions and effectively uniform over the region of interest. This has sometimes been taken to imply that the actual distribution of the inducing field can be ignored when calculating the induced currents and fields in the region considered. This assumption is implicit in the theory of the magnetotelluric method of geophysical prospecting given by Cagniard (1953). The limitations of results based on this theory are discussed in section 2.

Price (1964), in a comprehensive note on the interpretation of magnetic variations and magnetotelluric data, points out that a knowledge of the inducing field and surrounding ground conductivity in the immediate neighborhood of some particular station is not usually sufficient to determine the strength of the induced currents in that neighborhood. The induced currents are





affected by the distribution of the entire inducing field and by the average properties of the conductor over a region of corresponding dimensions. It is true that the entire induced current system will also contribute to the field at a particular station, but the largest contribution comes from induced currents in the immediate neighborhood. The important point is that not only the local properties, but the properties of the conductor as a whole determine the strength of the induced currents in the region of interest.

Price (1964) also points out that to approach the problem of the interpretation of local patterns of geomagnetic variations in an objective way, the variation fields should be separated into parts of external and internal origin and these parts should be examined separately. The anomalous patterns in the fields of the induced currents are produced by non-uniform distributions of conductivity in the earth, whereas the external inducing field is of a relatively simple form and varies only slightly over the anomalous area except near the equatorial and auroral electrojets. There seems to be no reason to suggest that the ionosphere has anomalous local properties, even though a small effect on the (non-isotropic) conductivity of the ionosphere might be



produced by a strong perturbation of the earth's magnetic field. Price (1964) suggests that even if a considerable disturbance is caused in the ionosphere by such local anomalies it is doubtful that the surface values of the magnetic field would be greatly affected. Also, if the external field is found to reflect to a small extent the anomalous magnetic field distribution, this can be attributed to the general mutual induction between the earth and the ionosphere.

Once the external field and its induced current system is known, the local problem reduces to examining the local redistribution of a given average system of induced currents caused by local inhomogeneities of conductivity. However, it is not necessarily a simple problem of redistribution of steady current flow, since the currents are time varying and therefore a skin effect will be encountered.

The mathematical problems which must be considered in this regard are those relating to the disturbance of skin effect distributions of current rather than actual electromagnetic induction problems. This type of mathematical problem is described by Price (1964) as follows:



"Using cartesian coordinates  $(x,y,z)$  with the  $z$  axis vertically downwards, a non-uniform conductor occupies the half-space  $z>0$ . Near the origin the conductivity is a function (not necessarily continuous) of  $(x,y,z)$ , but at great distances from the origin it is a function of  $z$  only. A given alternating e.m.f. impels currents near the surface of the conductor. [The problem is] to determine the distribution and surface field of these currents."

The electric field arises from a varying external magnetic field. This electric field is controlled not only by the external source but also by the properties and geometry of the conductor at great distances.

Problems of this sort can be solved for two-dimensional cases but when an attempt is made to reduce any problem involving electromagnetic induction of currents to a two-dimensional problem by supposing that conditions obtained in a limited region extend to infinity in two opposite directions, it is necessary to closely examine the conditions at infinity and ensure that they are acceptable.

The problems of electromagnetic induction dealt



with in this thesis are confined to two-dimensional problems with regard to both conductive geometry and field distribution.

### 1.3 The Two-Dimensional Problem

#### 1.3.a E and H Polarizations

The coordinate system is shown in Fig. 1.1. The region  $-|h| < z < 0$  is a free space region with conductivity equal to zero. A conductor occupies the half-space  $z > 0$  and it is assumed that a current source of some form is located at or above  $z = -|h|$ .

For an oscillating field with time dependence  $\exp(i\omega t)$  where  $\omega$  is the angular frequency and the period  $2\pi/\omega$  is sufficiently long so that displacement currents may be neglected, Maxwell's equations become:

$$\text{CURL } H = vE \quad (1.1)$$

$$\text{CURL } E = -i\omega uH \quad (1.2)$$

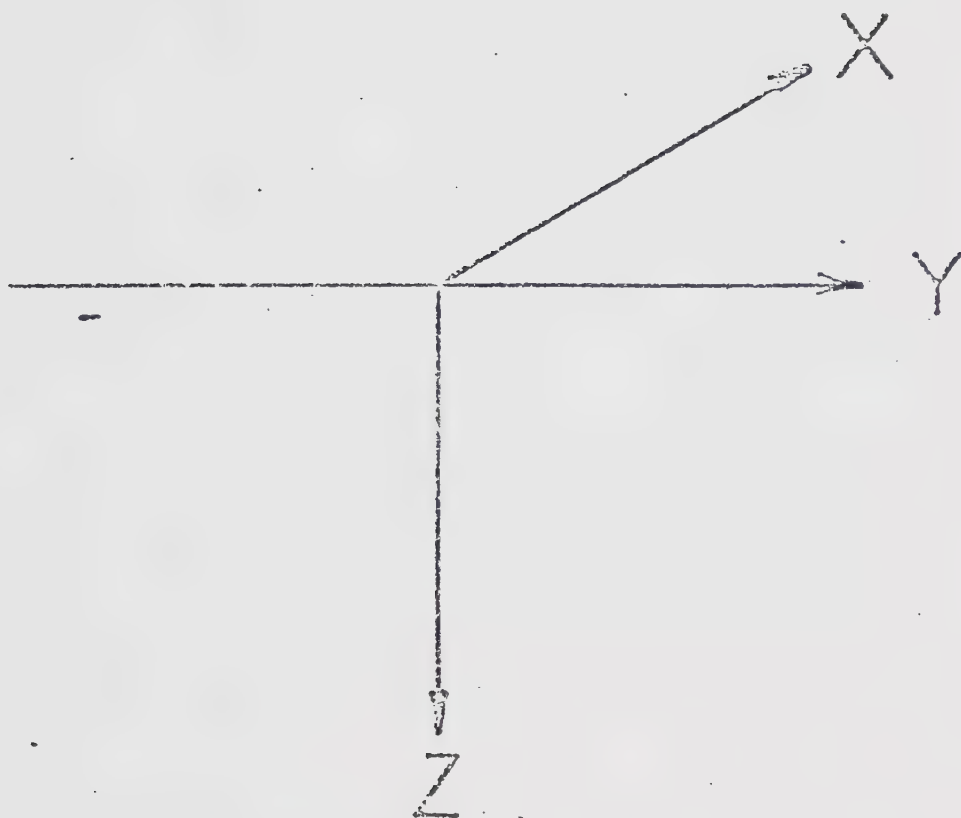
where  $v$  is the conductivity appropriate for each region,  $u$  is the magnetic permeability of free space and the time factor  $\exp(i\omega t)$  is understood in all field quantities.







Fig. 1.1      The coordinate system. X-Y plane represents  
the surface of the semi-inifinite half space  
conductor with a plane boundary.





In the two-dimensional problem the fields do not vary in one direction, in this case the x-direction. That is all quantities are independent of x, and Maxwell's equations reduce to

$$\partial H_z / \partial y - \partial H_y / \partial z = v E_x, \quad (1.3)$$

$$\partial H_x / \partial z = v E_y, \quad (1.4)$$

$$-\partial H_x / \partial y = v E_z, \quad (1.5)$$

$$\partial E_z / \partial y - \partial E_y / \partial z = i \omega \mu H_x, \quad (1.6)$$

$$\partial E_x / \partial z = -i \omega \mu H_y, \quad (1.7)$$

$$-\partial E_x / \partial y = -i \omega \mu H_z. \quad (1.8)$$

These equations are such that only  $E_x$ ,  $H_y$  and  $H_z$  are involved in (1.3, 1.7 and 1.8) and only  $H_x$ ,  $E_y$  and  $E_z$  are involved in (1.4, 1.5 and 1.6). These two separate sets of equations can therefore be solved independently. Combining (1.3), (1.7) and (1.8) we obtain

$$\partial^2 E_x / \partial y^2 + \partial^2 E_x / \partial z^2 = i \omega \mu v E_x \quad (1.9)$$

which is the equation to be solved in all regions for the E-polarization case (the case in which the electric field is parallel to any conductivity discontinuities).

Combining (1.4), (1.5) and (1.6) a similar equation is obtained for the H-polarization case (the case





in which the magnetic field is parallel to any conductivity discontinuities):

$$\partial^2 H_x / \partial y^2 + \partial^2 H_x / \partial z^2 = i\omega\mu v H_x. \quad (1.10)$$

With the proper values of  $v$  inserted for each conductive region, and with the proper boundary conditions, these equations can be solved for the separate cases to obtain the field distributions. For the E-polarization,  $E_x$  is determined from the solution of (1.9), and then (1.7) and (1.8) may be used to calculate the appropriate components. Also, for the H-polarization,  $H_x$  may be determined from (1.10), and equations (1.4) and (1.5) may be used to obtain the appropriate electric field components.

### 1.3.b Determinacy of the Two-Dimensional Problem

As mentioned in section 1.2.b not all two-dimensional problems are determinate. It is important, then, to examine the conditions for determinacy for a periodic inducing field over a semi-infinite uniform conductor with a plane boundary occupying the half-space  $z > 0$ . Following Price (1950), we let  $E_x$  be of the form



$$E_x = Z(z) \cdot Y(y) \cdot \exp(i\omega t), \quad (1.11)$$

and substitution of this expression for  $E_x$  into equation (1.9) gives:

$$\partial^2 Y / \partial y^2 = (1/Z) \cdot (i\omega \mu v Z - \partial^2 Z / \partial z^2) \cdot Y \quad (1.12)$$

for  $z > 0$ , and

$$\partial^2 Y / \partial y^2 = -(1/Z) \cdot (\partial^2 Z / \partial z^2) \cdot Y \quad (1.13)$$

for  $z < 0$ , where the arguments for  $Y$  and  $Z$  have now been dropped.

Since the coefficient of  $Y$  on the right of (1.12) and (1.13) is independent of  $x$  and  $y$  it must be a constant,  $-s^2$ , where  $s$  is real, positive and non-zero such that

$$\partial^2 Y / \partial y^2 = -s^2 Y. \quad (1.14)$$

Therefore, in the region  $z > 0$

$$\partial^2 Z / \partial z^2 - (i\omega \mu v + s^2) Z = 0 \quad (1.15)$$



and

$$Z(z) = A \cdot \exp(-pz) + B \cdot \exp(pz) \quad (1.16)$$

where  $p^2 = i\omega\mu + s^2$  and A and B are constants.

In the region  $z < 0$ ,

$$\partial^2 Z / \partial z^2 - s^2 Z = 0 \quad (1.17)$$

and

$$Z(z) = a \cdot \exp(-sz) + b \cdot \exp(sz), \quad (1.18)$$

where a and b are constants.

The corresponding E field is then

$$E_x = \{A \cdot \exp(-pz) + B \cdot \exp(pz)\} \cdot Y \quad (1.19)$$

for  $z > 0$ , and

$$E_x = \{a \cdot \exp(-sz) + b \cdot \exp(sz)\} \cdot Y \quad (1.20)$$

for  $z < 0$ .

As  $z$  becomes large,  $E_x$  must tend to zero so that



B must be zero. At the boundary  $z=0$ ,  $E_x$  must be continuous, and so

$$A = a + b. \quad (1.21)$$

The corresponding magnetic fields are obtained from (1.7) and (1.8) for  $z>0$ ;

$$H_y = (i/wu) \cdot (\partial E_x / \partial z) = -(ipA/wu) \cdot \exp(-pz) \cdot Y \quad (1.22)$$

$$H_z = -(i/wu) \cdot (\partial E_x / \partial y) = -(iA/wu) \cdot \exp(-pz) \cdot (\partial Y / \partial y); \quad (1.23)$$

and for  $z<0$ ;

$$H_y = -(is/wu) \cdot \{a \cdot \exp(-sz) - b \cdot \exp(sz)\} \cdot Y \quad (1.24)$$

$$H_z = -(i/wu) \cdot \{a \cdot \exp(-sz) + b \cdot \exp(sz)\} \cdot (\partial Y / \partial y). \quad (1.25)$$

The tangential component of the magnetic field must be continuous across the boundary  $z=0$ , which leads to the relation

$$pA = s(a-b). \quad (1.26)$$

The scalar potential  $\phi$  of the total magnetic field in the region  $-|h|<z<0$  satisfies Laplace's equation





and is of the form

$$\mathcal{E} = -\{C \cdot \exp(-sz) + D \cdot \exp(sz)\} \cdot P(y) \quad (1.27)$$

where  $P(y)$  satisfies the equation  $\partial^2 P(y) / \partial y^2 = -s^2 P(y)$ .

Since the conductivity outside the conductor is zero

$$\text{Curl } H = 0 \quad (1.28)$$

and  $H_y$  and  $H_z$  can be found from the relation

$$H = -\text{grad } \mathcal{E} \quad (1.29)$$

as:

$$H_y = \{C \cdot \exp(-sz) + D \cdot \exp(sz)\} \cdot (\partial P(y) / \partial y) \quad (1.30)$$

$$H_z = -s \cdot \{C \cdot \exp(-sz) - D \cdot \exp(sz)\} \cdot P(y). \quad (1.31)$$

Equating (1.24) and (1.30) gives:

$$-is_a/w_u = C \quad is_b/w_u = D \quad Y(y) = \partial P(y) / \partial y. \quad (1.32)$$

Combining (1.21), (1.26) and (1.32) gives:



$$D = \{(p-s)/(p+s)\} \cdot C, \quad (1.33)$$

$$a = \{(p+s)/(p-s)\} \cdot (iwu/s) \cdot D, \quad (1.34)$$

$$b = -\{(p-s)/(p+s)\} \cdot a, \quad (1.35)$$

and

$$A = -2sb/(p-s). \quad (1.36)$$

Therefore by specifying  $C$  all the other quantities will be determined. This analysis, while confined to uniform subsurfaces, can be extended to multi-layered cases.

The part of  $\mathcal{E}$  in (1.27) which involves  $\exp(-sz)$  corresponds to the inducing field of the current sources and the part which involves  $\exp(sz)$  corresponds to the field of the induced currents. It can be assumed that the inducing field potential is specified by the current distribution so that  $C \cdot \exp(-sz) \cdot P(y)$  is known. From the preceding discussion it can be seen that all other fields and potentials are determined from the inducing field. Therefore, the problem is determinate for  $s$  positive and non-zero. For  $s=0$  the problem becomes indeterminate in general as explained by Price (1950). The H-polarization can be shown to be determinate in the same manner.



#### 1.4 Methods for Solving the Two-Dimensional Problem

In his classic paper, Price (1950) considered electromagnetic induction in a semi-infinite conductor with a plane boundary for any inducing field. Cagniard (1953), in his derivation of the well known expression for apparent resistivity, considered a horizontally stratified earth and a uniform source. Wait (1954) and Price (1962) discussed Cagniard's results in terms of a source of finite dimensions. However, until the last decade, little attention has been paid to the problem of a vertical fault in the conductive region which represents the earth. It is well known that there are limited regions in various parts of the earth where temporal changes in the geomagnetic field at relatively near stations show considerable differences in form and amplitude. These differences remain consistent in character for the fluctuations of a given frequency, and form a definite pattern for the area studied. They are associated with lateral variations in conductivity below the earth's surface. It is important to understand the manner in which lateral variations affect the surface field in order to interpret such variations.

D'Erceville and Kunetz (1962) obtained a solution for two media of different conductivities in



contact along a vertical plane overlaying a horizontal basement that is either infinitely conducting, infinitely resistive or at infinite depth when the magnetic field is everywhere parallel to the strike of the fault, (H-polarization). Rankin (1962) extended this work in his study of "conductive" and "resistive" dikes.

Weaver (1963) considered a half-space conductor which consisted of two quarter-spaces of different conductivity with a plane vertical fault of infinite depth. He considered both the H-polarization case and the E-polarization case using an analytical technique. His H-polarization case agreed well with that of D'Erceville and Kunetz. However, in order for him to obtain a solution for the E-polarization case he found it necessary to use the approximate boundary condition that the tangential magnetic field is constant along the surface of the conductor. Recently, Mann (1970) has proposed a perturbation technique to consider the original Weaver (1963) problem, and has shown that Weaver's original solution is just a first approximation to the field inside the conductor for normally incident waves. Weaver and Thomson (1972) have applied this technique and have been able to avoid the approximate boundary condition of the constancy of the horizontal magnetic field along the





surface and have obtained approximate solutions.

In the meantime several numerical methods have been used to obtain solutions for problems with vertical discontinuities for both H-polarization and E-polarization cases. Dulaney and Madden (1962) were the first to apply the transmission line analogy over a two-dimensional mesh to such problems as these. This method has been used by many authors (including Madden and Thompson, 1965; Madden and Swift, 1969; Swift, 1967,1971; Wright, 1969,1970; and others). The finite element method, which uses the principle that electromagnetic fields behave in such a way as to minimize the energy, has recently been applied to induction problems by Coggon (1971), Ryu (1972) and Reddy and Rankin (1972). Finite difference techniques have been applied by Neves (1957), Latka (1966), Patrick and Bostick (1969) and others. Jones and Price (1969,1970,1971a,b) have employed the finite difference technique for studies of various two-dimensional conductivity distributions, and Jones and Pascoe (1971) and Pascoe and Jones (1972) have given a general computer program for the solution of the local perturbation problem.

Jones and Price (1969,1970) considered the half-



space conductor as the limit of a spherical conductor as the radius becomes infinite. They then carefully developed the boundary conditions and were able to obtain solutions for both the H-polarization and E-polarization cases. Jones and Price (1970) studied the field distribution within the whole two-dimensional region of interest, as well as the surface values of the various components, including the Cagniard (1953) apparent resistivity. In more recent work, Jones and Price (1971a,b) and Jones (1971a,b) as well as Hibbs and Jones (1972a) have calculated apparent resistivity values along the surface of the conductor.

It should be noted that in all the numerical methods mentioned above the assumption has been made that the inducing field is uniform. A non-uniform source in the form of a line current has been considered by Wait (1962), Dosso and Jacobs (1968) and others. Schmucker (1971) has considered non-uniform sources over a laterally inhomogeneous earth in which the lateral changes in conductivity are confined to a limited depth range. Hermance and Peltier (1970) studied the magnetotelluric field of a line current over a layered subsurface, and later (Peltier and Hermance, (1971)) extended their approach to include symmetric current distributions, such



as a Gaussian current intensity source.

One aspect of the work of this thesis has been to combine the method of Peltier and Hermance (1971) with the iterative finite difference method of Jones and Price (1970) to investigate embedded conductivity inhomogeneities for symmetric non-uniform sources, as well as for non-symmetric current source distributions. Two papers (Hibbs and Jones, 1972b,c) describe this work and it is further discussed in the following sections.

It should be emphasized here that the E-polarization case is readily adaptable to such an approach, whereas the H-polarization case is not. Consequently, work of this thesis is primarily concerned with the two-dimensional E-polarization case.



## 2. SOURCE DISCUSSION

Cagniard (1953), in his classic paper presenting the basic ideas underlying a prospecting method using magnetotelluric techniques, assumed that natural oscillating electromagnetic fields near the earth's surface are uniform. Consequently, the amplitude and phase relationships of the horizontal components of E and H over a layered conductor depended upon the electrical conductivities of the strata and the period of the oscillating field. The apparent resistivity in ohm-m is given by

$$\rho_A = 0.2T (E/H)^2 \quad (2.1)$$

where T is the period in seconds, and E (in millivolts/km.) and H (in gammas) are mutually perpendicular electric and magnetic field components at the surface of the earth. Cagniard (1953) presented master curves of apparent resistivity for various layered conductors and a method of interpretation of experimental magnetotelluric data from the master curves was given.

In his original paper Cagniard (1953) did not explain the origin of the earth currents but only required that they be uniform. Later, in correspondence with Wait (which is reproduced following the paper by Wait, 1954)





Cagniard stated that the magnetotelluric perturbations are caused by vast systems of ionospheric currents whose dimensions are on a global scale.

Since the depth of penetration of induced currents depends upon the period, by using one observing station the magnetotelluric method is able to indicate the conductivity distribution with depth (over a suitable range of frequencies) and a conductivity profile can be deduced. However, if the source field is non-uniform, the influence of such non-uniform source field distributions should be studied in relation to the magnetotelluric method. It is apparent that over some regions of the earth, for example near the magnetic equator (Forbush and Casaverde, 1961) and near the auroral oval (Kisabeth and Rostoker, 1971), the inducing field is not always uniform.

Aside from the discussion by Wait (1954), little attention has been paid to Cagniard's fundamental assumption that the electromagnetic field is uniform over any horizontal plane. Wait (1954) showed that if this condition is not satisfied Cagniard's calculation of the quantity  $E/H$  is not exact.

From calculated corrections to this quantity involving the second-order spatial derivative, Wait



concluded that the corrections would be necessary if the magnetic field changed appreciably in a distance of 35 km. for periods greater than 10 seconds and ground conductivity of the order of  $10^{-3}$  ohm/m. Wait also observed that if the source field was generated by ionospheric currents flowing at heights of about 100 km. the corrections would be important for many of the geomagnetic oscillations used in magnetotelluric methods. This is particularly true of geomagnetic fluctuations observed in connection with the fields of auroral and equatorial electrojets.

As mentioned before, Cagniard argued in his reply to Wait that the magnetotelluric perturbations are produced by vast current systems whose electric fields have global dimensions, and therefore his equations could be applied in most cases. This conclusion is fairly reasonable for the source fields considered by Wait. However, Wait himself made a simplifying assumption in that he considered a semi-infinite conductor of uniform conductivity. For a conductor whose conductivity varies with depth it is found (Price, 1962) that the dimensions of the source field cannot be ignored even if the field is of global dimensions and the skin depth of the inducing field is moderate.



Price (1962) outlined the general theory of magnetotelluric methods including source field considerations and applied this theory to a simple case to show the importance of the spatial dimensions of the source. He estimated the spatial wave number  $s$  of the source field and concluded that the least value of  $s$  can be obtained by equating  $2\pi/s$  to the circumference of the earth, which corresponds to the wavelength of a field representing a spherical harmonic of the first order, which gives  $s=1.57 \times 10^{-9} \text{ cm}^{-1}$ . Most geomagnetic fields could contain spherical harmonics of a higher order than this, and a more representative value would be  $s=1.0 \times 10^{-8} \text{ cm}^{-1}$ . More localized fields such as those of an ionospheric electrojet contain spherical harmonics of an even higher order. Price suggests that a representative value of  $s$  could be found by equating  $2\pi/s$  to four times the height (approximately 100 km.) of the ionospheric currents. The maximum value of  $s$  is thus approximately  $1.57 \times 10^{-7} \text{ cm}^{-1}$ . Thus the values of  $s$  of most interest in magnetotelluric investigations lie between  $1.57 \times 10^{-9} \text{ cm}^{-1}$  and  $1.57 \times 10^{-7} \text{ cm}^{-1}$ .

Price (1962) then showed, that for certain distributions of subsurface conductivity, the quantity



$E_x/H_y$  can be considerably affected by the value of  $s$ . One simple case which he chose was that in which the conductor has a constant conductivity  $v$  down to a certain depth  $D$  and zero conductivity below. The quantity  $E_x/H_y$  was found to be

$$E_x/H_y = (iw/p) \cdot \{ [p+s+(p-s) \cdot \exp(-2pD)] / [p+s-(p-s) \cdot \exp(-2pD)] \} \quad (2.2)$$

where  $p^2 = s^2 + iwuv$ .

From this it is seen that the ratio  $E_x/H_y$  depends upon  $s$ , both explicitly on the right hand side of (2.2) and in the quantity  $p$  as well. When  $s=0$ , which corresponds to a uniform source field,

$$E_x/H_y = (iw/p \bullet) \cdot \{ [1 + \exp(-2p \bullet D)] / [1 - \exp(-2p \bullet D)] \} \quad (2.3)$$

where  $p \bullet = \sqrt{iwuv}$ .

When  $D$  is infinite, that is for a semi-infinite conductor, equation (2.2) reduces to

$$E_x/H_y = iw/p \quad (2.4)$$

and so for this case there is a dependence on  $s$ .





With a first layer resistivity of 1000 ohm-m at a period of 100 seconds, the amplitude of  $|E_x/i\omega H_y|$  was found by Price (1962) to vary greatly with spatial wave number  $s$  which itself varies over the range  $1.57 \times 10^{-9} \text{ cm}^{-1}$  to  $1.57 \times 10^{-7} \text{ cm}^{-1}$ . This was particularly evident when the thickness of the first layer of the conductor was less than 10 km. A complete description of this phenomenon is given by Price (1962).

Although the foregoing calculations were made for a simple distribution of conductivity, they show that the dimensions of the source field can be an important influence on the quantity  $|E_x/i\omega H_y|$ . This is true not only for local fields but also for fields with global dimensions. It should be pointed out also that the above discussion deals with sources of a single wave number whereas sources in general contain many wave numbers. The sources investigated in the remainder of this thesis will deal with the latter more general type.



### 3. SOLUTIONS FOR NON-UNIFORM SOURCES

#### 3.1 Two-Dimensional Solutions for Non-Uniform Sources over Layered Media

##### 3.1.a Line Current Source

Hermance and Peltier (1970) investigated the magnetotelluric fields of a line current over a layered, two-dimensional earth. The line current flowed at a height of  $z = -|h|$  parallel to the  $x$  axis of Fig 3.1 with a sinusoidal time dependence  $\exp(i\omega t)$ . The E-polarization case is the applicable two-dimensional problem in this regard, and for this case the equation to be solved is given by (1.9). By the method of separation of variables, solutions of the form  $E_x(y, z) = Y(y)Z(z)$  are obtained, where

$$Y(y) = C(s) \cdot \cos(sy) + D(s) \cdot \sin(sy), \quad (3.1)$$

$$Z(z) = A_n(P) \cdot \exp(-Pz) + B_n(P) \cdot \exp(Pz), \quad (3.2)$$

and  $P^2 = s^2 + i\omega\mu_0 V_n$ .

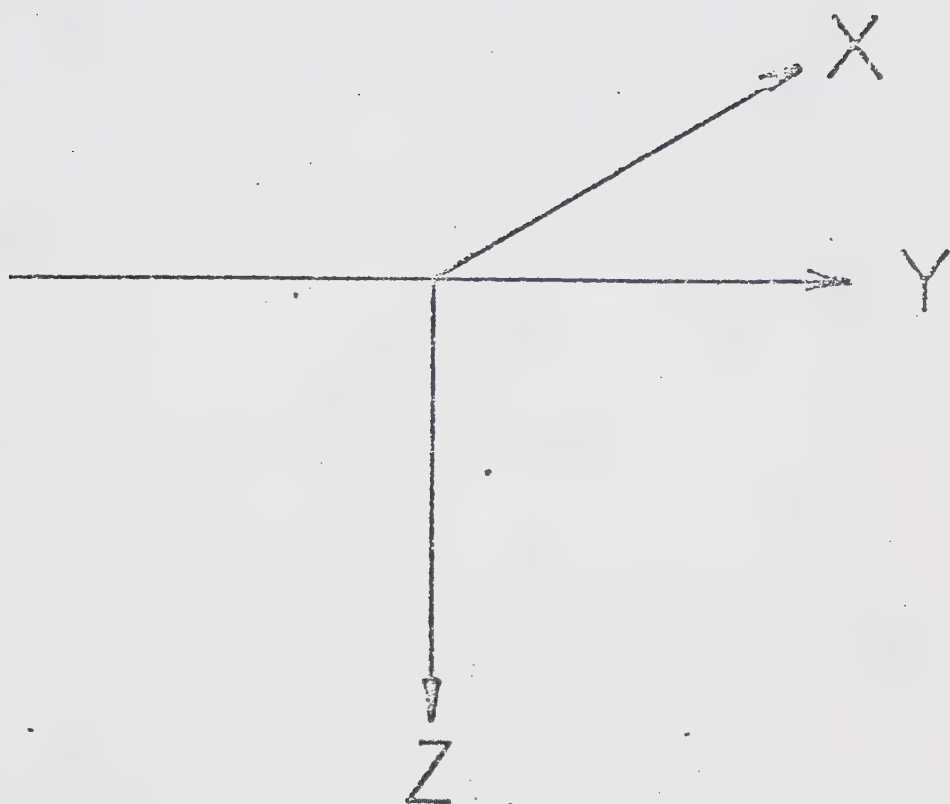
The values of  $s$  and  $V_n$  are the spatial wave number and the homogeneous conductivity of the  $n$ th layer respectively.

Due to the position of the line current the





Fig. 3.1      The coordinate system.







electric field is an even function of  $y$ . Therefore only the cosine term of (3.1) need be considered.

In the space above the conductor the conductivity is zero and  $P_1=s$ . If  $A_1(P)=1$ , then  $C(s)$  is a frequency dependent parameter which characterizes the source.  $B_1(P)$  can be thought of as a reflection coefficient which represents the contributions to the total field from subsurface layers ( $z>0$ ). From the above discussion the elementary electric field in the first layer is

$$E_x(y,z) = \{ \exp(-sz) + B_1(P) \cdot \exp(sz) \} \cdot C(s) \cdot \cos(sy), \quad (3.3)$$

The actual field components are synthesized from the elementary fields by the use of the Fourier integral:

$$E_x(y,z) = \int_0^{\infty} \{ \exp(-sz) + B_1(P) \cdot \exp(sz) \} \cdot C(s) \cdot \cos(sy) \, ds. \quad (3.4)$$

By taking the curl of (3.4) and applying Maxwell's equations the magnetic field components are found:

$$H_y(y,z) = -(i/wu) \cdot \int_0^{\infty} s \cdot \{ \exp(-sz) - B_1(P) \cdot \exp(sz) \}$$



$$.C(s) \cdot \cos(sy) \, ds, \quad (3.5)$$

$$H_z(y, z) = (i/wu) \cdot \int_0^\infty s \cdot \{\exp(-sz) + B_1(P) \cdot \exp(sz)\} \\ \cdot C(s) \cdot \sin(sy) \, ds. \quad (3.6)$$

If the contribution from the subsurface layers is neglected by setting  $B_1(P) = 0$ , then a line current at  $z^0 = -h$  has a horizontal magnetic field given by:

$$H_y = -(I \cdot / 2\pi) \cdot (z - z^0) / (y^2 + (z - z^0)^2) \quad (3.7)$$

where  $I \cdot$  is the line current intensity.

Setting (3.5) equal to (3.7) gives

$$-(i/wu) \cdot \int_0^\infty s \cdot \exp(-sz) \cdot C(s) \cdot \cos(sy) \, ds \\ = -(I \cdot / 2\pi) \cdot (z - z^0) / (y^2 + (z - z^0)^2). \quad (3.8)$$

from Laplace transform tables (Erdelyi et al., 1961)

$$\int_0^\infty \exp(-[z - z^0]s) \cdot \cos(sy) \, ds = (z - z^0) / (y^2 + [z - z^0]^2), \quad (3.9)$$

and combining (3.8) and (3.9) and solving for  $C(s)$  gives:

$$C(s) = -(i w u I \cdot / 2\pi) \cdot (\exp(z^0 s) / s). \quad (3.10)$$

The remaining unknown  $B_n(P)$  can be determined by



applying the boundary conditions that the horizontal electric and magnetic fields are continuous across the interfaces between the conductive layers. For a two layered earth  $B(P)$  must be zero in order that  $Ey^3$  does not become infinite with depth. These conditions give:

$$B_1(P) = (R-1)/(R+1), \quad (3.11)$$

where

$$R = s(Q+1)/\{P_2 \cdot (Q-1)\}, \quad (3.12)$$

and

$$Q = \{(P_2 + P_3)/P_2 - P_3\} \cdot \exp(2P_2 d), \quad (3.13)$$

where  $d$  is the thickness of the first layer of the conductor.

The relations for the electromagnetic field components for the first layer (3.4), (3.5), and (3.6) can then be numerically integrated on a digital computer using Filon's Method (Tranter 1956). The observed value of any field component is then obtained by taking the real part of the product of the field component and the time



dependence  $\exp(i\omega t)$ .

By varying the height of the line current, Hermance and Peltier (1970) concluded (with some reservations) that for an 'average continental' crust Cagniard's magnetotelluric method is applicable if the electrojet can be represented by a line current at a height greater than 500 km., or by a broad current distribution at lower altitude. However, Hermance and Peltier (1970) felt that more extensive research into the validity of these restrictions would have to be undertaken, and concurred with Price (1962), Wait (1962), Ward and Morrison (1966), Rikitake (1966) and Madden and Swift (1969) that the current source structure could not in general be ignored. Magnetotelluric measurements over tectonically active regions where highly conductive regions occur at depths of less than 25 km. were found to be much less susceptible to source effects, and therefore in these regions Cagniard's method could be applied (Hermance and Peltier, 1970). These observations are restricted to layered earth models and the source effect could be enhanced by lateral inhomogeneities in the conductivity configuration of the model.

### 3.1.b Gaussian Current Source





As an extension of their work on line current sources Feltier and Hermance (1971) considered a laterally diffuse current distribution. The electrojet was simulated by a continuum of weighted line current elements whose fields were superimposed to obtain the total field. An infinitesimally thin current sheet at a height of  $z = -|h| = -110$  km. represented the source. The distribution of the current intensity was taken to be Gaussian and characterized by a standard deviation of 240 km. and the time dependence was sinusoidal.

Since the current distribution is symmetric with respect to the origin, the electric field is again an even function of  $y$ . Following the same discussion as previously, which led to (3.3), the elementary electric field in the first layer is

$$E_x(y, z) = \{ \exp(-sz) + B_1(P) \cdot \exp(sz) \} \cdot C(s) \cdot \cos(sy). \quad (3.14)$$

$B(P)$  is defined by (3.11) through (3.13) for a two layered earth and  $C(s)$  is obtained for a line current as before:

$$C(s) = - \{ (i\omega I_0) / 2\pi \} \cdot (\exp(z_0 s) / s). \quad (3.15)$$



The Gaussian current distribution can be represented as a function of  $y$

$$I(y) = I_0 \cdot \exp(-y^2/2k^2) \quad (3.16)$$

where  $I_0$  and  $k$  are the current intensity directly above the origin and the standard deviation respectively. If it is assumed that the source is a composite of elemental line sources with an intensity distribution described by (3.16), then the horizontal magnetic field intensity due to an elemental line source at  $(y^0, z^0)$  can be written as:

$$H_{y^1}(\text{element}) = -(I_0/2\pi) \cdot \exp(-[y^0]^2/2k^2) \cdot (z-z^0) / \{(z-z^0)^2 + (y-y^0)^2\}. \quad (3.17)$$

The total horizontal magnetic field is obtained by integrating over all values of  $y^0$  and is

$$H_{y^1}(\text{total}) = -(I_0/2\pi) \cdot \int_{-\infty}^{\infty} \{\exp(-[y^0]^2/2k^2) \cdot (z-z^0) / [(z-z^0)^2 + (y-y^0)^2]\} dy^0. \quad (3.18)$$

The Gaussian source constant  $G(s)$  is obtained in the same manner as  $C(s)$ :



$$\begin{aligned}
-(i/wu) \cdot \int_0^{\infty} s \cdot \exp(-sz) \cdot G(s) \cdot \cos(sy) \, ds = -(I \bullet / 2\pi) \cdot \\
\int_{-\infty}^{\infty} \{ \exp(-[y^0]^2 / 2k^2) \cdot (z - z^0) \\
/ [(z - z^0)^2 + (y - y^0)^2] \} \, dy^0.
\end{aligned} \tag{3.19}$$

If in (3.9)  $y$  is replaced by  $(y - y^0)$  and both sides are multiplied by  $\exp(-[y^0]^2 / 2k^2)$  and the expressions are integrated over all  $y^0$ , then

$$\begin{aligned}
-(i/wu) \cdot \int_{-\infty}^{\infty} \int_0^{\infty} s \cdot \exp(-sz) \cdot C(s) \cdot \cos(s[y - y^0]) \\
\cdot \exp(-[y^0]^2 / 2k^2) \, ds \, dy^0 = -(I \bullet / 2\pi) \\
\cdot \int_{-\infty}^{\infty} \{ \exp(-[y^0]^2 / 2k^2) \cdot (z - z^0) \\
/ [(z - z^0)^2 + (y - y^0)^2] \} \, dy^0
\end{aligned} \tag{3.20}$$

and comparison of (3.19) and (3.20) gives

$$\begin{aligned}
C(s) \int_{-\infty}^{\infty} \exp(-[y^0]^2 / 2k^2) \cdot \cos(s[y - y^0]) \, dy^0 = G(s) \\
\cdot \cos(sy).
\end{aligned} \tag{3.21}$$

By solving for  $G(s)$  we have

$$G(s) = \sqrt{2\pi} k \cdot \exp(-s^2 k^2 / 2) \cdot C(s), \tag{3.22}$$

and therefore

$$G(s) = -(i I \bullet w u k / \sqrt{2\pi} \cdot s) \cdot \exp(s z^0 - s^2 k^2 / 2). \tag{3.23}$$



The electromagnetic field components for the first layer are obtained by substituting  $G(s)$  for  $C(s)$  in (3.4), (3.5) and (3.6).

Again through numerical integration on a digital computer by Filon's method the actual field components may be obtained. The observed values of the field components are obtained as in 3.1.a.

From the results of this work Peltier and Hermance (1971) concluded that the most pronounced source effect occurs over continental areas where layers of low resistivity overlay those of high resistivity. Over this type of conductor it was concluded that the conventional Cagniard method might lead to serious errors in interpretation. Also, it is possible that the presence of lateral inhomogeneities in the conductivity structure could enhance the effect of the non-uniform source. However, they found that the source effect for all two layer models in which a high resistivity surface layer overlies a lower resistivity layer is diminished for the Gaussian source distribution.

### 3.2. Two-Dimensional Solutions for Non-Uniform Sources over Laterally Inhomogeneous Media





### 3.2.a Iterative Solutions

The primary limitation of the method of solution in the preceding sections 3.1.a and 3.1.b is that the conducting medium must be laterally homogeneous. While the solution for only two specific source configurations were obtained, other symmetric source configurations can be calculated and the method can be extended to non-symmetric sources as will be shown in section 4.1. The solution for laterally inhomogeneous conductivity structures with finite conductivities can best be obtained through the use of the finite difference method. The non-uniformity of the source is reflected in the boundary values supplied to the finite difference mesh. A complete discussion of the boundary conditions will be given in section 3.2.b.

Jones and Pascoe (1971) presented an iterative finite difference method for dealing with an embedded two-dimensional anomaly of arbitrary shape. This work was an extension to the method developed by Jones and Price (1970, 1971a,b) who considered several particular laterally inhomogeneous conducting regions. The method involves the solution of the appropriate finite difference



equations over a mesh of grid points by the Gauss-Seidel iterative technique (Smith, 1969). The general model is illustrated in Fig. 3.2 along with the coordinate system. The grid size is variable and the surface is taken as the line between the region of conductivity A, which is a free space region, and the region of conductivity B. Anomalous conductivity regions which may be of arbitrary shape are represented here by the different letters.

The equation to be solved in all regions for the E-polarization case is of the form

$$\nabla^2 E_x = i n^2 E_x \quad (3.24)$$

where  $n^2 = 4\pi\omega\epsilon$ .

If  $E_x = f + ig$  then

$$\nabla^2 f + i \nabla^2 g = i n^2 f - n^2 g \quad (3.25)$$

and equating real and imaginary parts gives:

$$\nabla^2 f = -n^2 g \quad (3.26)$$

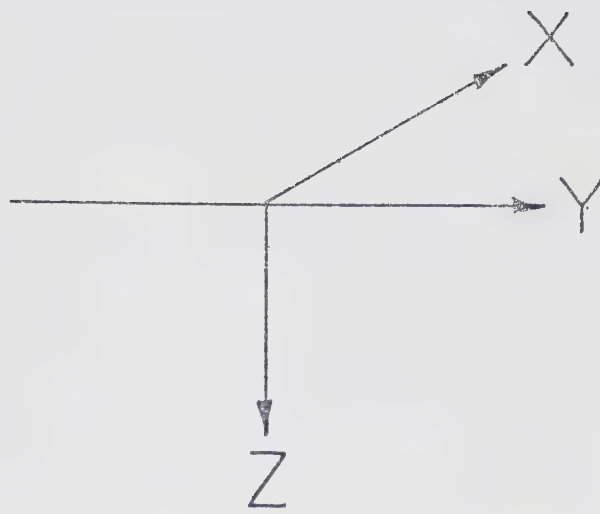
$$\nabla^2 g = n^2 f. \quad (3.27)$$

If a small region of the mesh is considered as





Fig. 3.2      The general two-dimensional model and  
coordinate system.    (After Jones and Pascoe,  
1971.)



A	A	A	A	A	A	A	A
A	A	A	A	A	A	A	A
A	A	A	A	A	A	A	A
A	A	A	A	A	A	A	A
B	B	B	B	B	B	B	B
B	B	B	B	B	B	B	B
B	B	C	C	D	D	B	B
B	B	C	C	E	E	B	B
B	B	F	F	E	E	B	B
B	B	B	B	B	B	B	B
B	B	B	B	B	B	B	B





illustrated in Fig. 3.3, (3.26) and (3.27) must be satisfied at each point, and in particular at point "0". Four conductivities occupy the quadrants surrounding the point "0". The mesh sizes vary, and in general  $d^1 \neq d^2 \neq d^3 \neq d^4$ . At the point "0" (3.26) and (3.27) become:

$$(\nabla^2 f)^0 = (-n^2 g)^0 \quad (3.28)$$

and

$$(\nabla^2 g)^0 = (n^2 f)^0. \quad (3.29)$$

A pair of finite difference equations is obtained by making use of Taylor's Theorem which yields

$$\begin{aligned} f^1 = f^0 + (\partial f / \partial y)^0 \cdot d^1 + (1/2) (\partial^2 f / \partial y^2)^0 \\ \cdot (d^1)^2 + \dots \end{aligned} \quad (3.30)$$

$$\begin{aligned} f^2 = f^0 + (\partial f / \partial z)^0 \cdot d^2 + (1/2) (\partial^2 f / \partial z^2)^0 \\ \cdot (d^2)^2 + \dots \end{aligned} \quad (3.31)$$

$$\begin{aligned} f^3 = f^0 - (\partial f / \partial y)^0 \cdot d^3 + (1/2) (\partial^2 f / \partial y^2)^0 \\ \cdot (d^3)^2 + \dots \end{aligned} \quad (3.32)$$

$$\begin{aligned} f^4 = f^0 - (\partial f / \partial z)^0 \cdot d^4 + (1/2) (\partial^2 f / \partial z^2)^0 \\ \cdot (d^4)^2 + \dots \end{aligned} \quad (3.33)$$

and similar equations for  $g^1, g^2, g^3, g^4$ .

If higher order terms are neglected, equations





Fig. 3.3      Notation used for grid points, dimensions and  
conductivities of the regions surrounding  
point '0'.    (After Jones and Pascoe, 1971.)





(3.28) and (3.29) can be expressed as a pair of finite difference equations:

$$\begin{aligned}
 f^0 \{1/(d^1)^2 + 1/(d^2)^2 + 1/(d^3)^2 + 1/(d^4)^2\} - n^2 g^0 = \\
 f^1 \cdot \{1/(d^1)^2 + [1/(d^1 + d^3)] \cdot (1/d^3 - 1/d^1)\} + \\
 f^2 \cdot \{1/(d^2)^2 + [1/(d^2 + d^4)] \cdot (1/d^4 - 1/d^2)\} + \\
 f^3 \cdot \{1/(d^3)^2 + [1/(d^1 + d^3)] \cdot (1/d^1 - 1/d^3)\} + \\
 f^4 \cdot \{1/(d^4)^2 + [1/(d^2 + d^4)] \cdot (1/d^2 - 1/d^4)\} \quad (3.34)
 \end{aligned}$$

or

$$f^0 \cdot \left( \sum_i 1/[d^i]^2 \right) - n^2 g^0 = f^1 D^1 + f^2 D^2 + f^3 D^3 + f^4 D^4 \quad (3.35)$$

where

$$D^1 = 1/(d^1)^2 + [1/(d^1 + d^3)] \cdot (1/d^3 - 1/d^1), \quad (3.36)$$

$$D^2 = 1/(d^2)^2 + [1/(d^2 + d^4)] \cdot (1/d^4 - 1/d^2), \quad (3.37)$$

$$D^3 = 1/(d^3)^2 + [1/(d^1 + d^3)] \cdot (1/d^1 - 1/d^3), \quad (3.38)$$

$$D^4 = 1/(d^4)^2 + [1/(d^2 + d^4)] \cdot (1/d^2 - 1/d^4). \quad (3.39)$$

A similar equation can be written for the  $g$  values:

$$\begin{aligned}
 g^0 \cdot \left( \sum_i 1/[d^i]^2 \right) + n^2 f^0 = g^1 D^1 + g^2 D^2 + g^3 D^3 \\
 + g^4 D^4. \quad (3.40)
 \end{aligned}$$





Equations (3.35) and (3.40) must be satisfied at each interior point of each region. These two equations can be solved simultaneously at point "0" for  $f^0$  and  $g^0$  where up-to-date values of  $f^i$  and  $g^i$  are obtained from the previous iteration. Equations (3.35) and (3.40) must hold for each of the surrounding regions.

That is:

$$f^{10} \left( \sum_i 1/[d^i]^2 \right) - (n^1)^2 \cdot g^{10} = f^{11}D^1 + f^{12}D^2 + \underline{f^{13}}D^3 + \underline{f^{14}}D^4 \quad (3.41)$$

$$f^{20} \left( \sum_i 1/[d^i]^2 \right) - (n^2)^2 \cdot g^{20} = \underline{f^{21}}D^1 + f^{22}D^2 + f^{23}D^3 + \underline{f^{24}}D^4 \quad (3.42)$$

$$f^{30} \left( \sum_i 1/[d^i]^2 \right) - (n^3)^2 \cdot g^{30} = \underline{f^{31}}D^1 + \underline{f^{32}}D^2 + f^{33}D^3 + f^{34}D^4 \quad (3.43)$$

$$f^{40} \left( \sum_i 1/[d^i]^2 \right) - (n^4)^2 \cdot g^{40} = f^{41}D^1 + \underline{f^{42}}D^2 + \underline{f^{43}}D^3 + f^{44}D^4 \quad (3.44)$$

$$g^{10} \left( \sum_i 1/[d^i]^2 \right) + (n^1)^2 \cdot f^{10} = g^{11}D^1 + g^{12}D^2 + \underline{g^{13}}D^3 + \underline{g^{14}}D^4 \quad (3.45)$$

$$g^{20} \left( \sum_i 1/[d^i]^2 \right) + (n^2)^2 \cdot f^{20} = \underline{g^{21}}D^1 + g^{22}D^2 + g^{23}D^3 + \underline{g^{24}}D^4 \quad (3.46)$$

$$g^{30} \left( \sum_i 1/[d^i]^2 \right) + (n^3)^2 \cdot f^{30} = \underline{g^{31}}D^1 + \underline{g^{32}}D^2 + g^{33}D^3 + g^{34}D^4 \quad (3.47)$$

$$g^{40} \left( \sum_i 1/[d^i]^2 \right) + (n^4)^2 \cdot f^{40} = g^{41}D^1 + \underline{g^{42}}D^2 + \underline{g^{43}}D^3 + g^{44}D^4 \quad (3.48)$$



where the first superscript indicates the conductive region considered and the second superscript refers to the particular point of interest. The underlined values are "fictitious" values and the boundary conditions for the interfaces between the regions of different conductivity allow these values to be expressed in terms of known values.

The internal boundary conditions for the E-polarization case are that both the tangential and normal components of  $H$  are continuous across any interface. These two components may be expressed in terms of  $E_x$  from equations (1.7) and (1.8).

$$H_y = (i/w) \cdot (\partial f / \partial z) - (1/w) \cdot (\partial g / \partial z) \quad (3.49)$$

and

$$H_z = -(i/w) (\partial f / \partial y) + (1/w) (\partial g / \partial y). \quad (3.50)$$

The condition for continuity of the tangential components applied to each boundary leads to the finite difference equations:

$$\underline{f_{13}} - f_{10} = f_{23} - f_{20} \quad \underline{g_{13}} - g_{10} = g_{23} - g_{20}$$



$$\begin{array}{ll}
\underline{f_{21}} - f^{20} = f^{11} - f^{10} & \underline{g_{21}} - g^{20} = g^{11} - g^{10} \\
\underline{f_{31}} - f^{30} = f^{41} - f^{40} & \underline{g_{31}} - g^{30} = g^{41} - g^{40} \\
\underline{f_{43}} - f^{40} = f^{33} - f^{30} & \underline{g_{43}} - g^{40} = g^{33} - g^{30} \\
\underline{f_{14}} - f^{10} = f^{44} - f^{40} & \underline{g_{14}} - g^{10} = g^{44} - g^{40} \\
\underline{f_{24}} - f^{20} = f^{34} - f^{30} & \underline{g_{24}} - g^{20} = g^{34} - g^{30} \\
\underline{f_{32}} - f^{30} = f^{22} - f^{20} & \underline{g_{32}} - g^{30} = g^{22} - g^{20} \\
\underline{f_{42}} - f^{40} = f^{12} - f^{10} & \underline{g_{42}} - g^{40} = g^{12} - g^{10}.
\end{array} \quad (3.51)$$

These equations allow us to express the fictitious values of (3.41) to (3.48) in terms of known values. Adding (3.41), (3.42), (3.43) and (3.44) and making use of the fact that

$$f^{ab} = f^b \quad (3.52)$$

$$g^{ab} = g^b \quad (3.53)$$

we obtain

$$Af^0 + Bg^0 = f^1C^1 + f^2C^2 + f^3C^3 + f^4C^4. \quad (3.54)$$

Similarly, adding (3.45), (3.46), (3.47) and (3.48) we obtain



$$-Bf^0 + Ag^0 = g^1C^1 + g^2C^2 + g^3C^3 + g^4C^4 \quad (3.55)$$

where

$$A = 4 \sum_i 1/(d^i)^2 \quad (3.56)$$

$$B = - \sum_i n^i{}^2 \quad (3.57)$$

$$C^1 = 4D^1 \quad (3.58)$$

$$C^2 = 4D^2 \quad (3.59)$$

$$C^3 = 4D^3 \quad (3.60)$$

$$C^4 = 4D^4. \quad (3.61)$$

Equations (3.54) and (3.55) are simultaneous equations which must be solved for  $f^0$  and  $g^0$ .

The observed electric field  $E(\text{obs})$  can be obtained by multiplying  $E_x$  by the time dependence  $\exp(i\omega t)$  and taking the real part of the result. This gives

$$E_x(\text{obs}) = \text{Re} [(f+ig)\exp(i\omega t)] = f.\cos(\omega t) - g.\sin(\omega t). \quad (3.62)$$

Similarly for the magnetic field components:





$$\begin{aligned}
H_y(\text{obs}) &= \text{Re} \left[ (i/w) \cdot (\partial E_x / \partial z) \right] \\
&= -(1/w) \cdot \{ (\partial f / \partial z) \cdot \sin(wt) + (\partial g / \partial z) \cdot \cos(wt) \},
\end{aligned}
\tag{3.63}$$

$$\begin{aligned}
H_z(\text{obs}) &= \text{Re} \left[ (-i/w) \cdot (\partial E_x / \partial y) \right] \\
&= (1/w) \cdot \{ (\partial f / \partial y) \cdot \sin(wt) + (\partial g / \partial y) \cdot \cos(wt) \}.
\end{aligned}
\tag{3.64}$$

The phases of these three components may be calculated as follows:

$$\begin{aligned}
\text{Phase of } E_x(\text{obs}) &= \text{Arctan} \{ [ f \cdot \sin(wt) + g \cdot \cos(wt) ] \\
&\quad / [ f \cdot \cos(wt) - g \cdot \sin(wt) ] \},
\end{aligned}
\tag{3.65}$$

$$\begin{aligned}
\text{Phase of } H_y(\text{obs}) &= \text{Arctan} \{ [ (\partial f / \partial z) \cdot \cos(wt) \\
&\quad - (\partial g / \partial z) \cdot \sin(wt) ] / [ -(\partial f / \partial z) \cdot \sin(wt) \\
&\quad - (\partial g / \partial z) \cdot \cos(wt) ] \},
\end{aligned}
\tag{3.66}$$

$$\begin{aligned}
\text{Phase of } H_z(\text{obs}) &= \text{Arctan} \{ [ -(\partial f / \partial y) \cdot \cos(wt) \\
&\quad - (\partial g / \partial y) \cdot \sin(wt) ] / [ (\partial f / \partial y) \cdot \sin(wt) \\
&\quad + (\partial g / \partial y) \cdot \cos(wt) ] \}.
\end{aligned}
\tag{3.67}$$

### 3.2.b Combined Solution for Non-Uniform Source and Laterally Non-Uniform Subsurface



From the method of Peltier and Hermance (1971), the electric field due to a symmetric non-uniform source over a horizontally layered earth may be calculated at any point  $(y,z)$  where  $-\infty < y < +\infty$  and  $z > -|h|$ . Values taken from such calculations may be used to give the boundary values in the Jones and Price (1970) and Jones and Pascoe (1971) iterative method of solving for the fields associated with lateral inhomogeneities in conductivity.

When the two methods are combined, the conductivity configuration must have identical layering at both boundaries for  $|y|$  large, since the Peltier and Hermance method applies only for a horizontally layered earth. Also, the anomalous conductivity region should be approximately three skin depths of the surrounding medium from the bottom and side boundaries. This latter point has been discussed by Pascoe and Jones (1972). When considering the location for the upper boundary of the finite difference mesh in the numerical method it is desirable to place it at such a height that any perturbations due to lateral inhomogeneities are negligible and such that it is below any ionospheric conductive region. In the work that follows the current source is chosen at  $z = -110$  km., and the upper boundary of the finite difference grid at  $z = -50$  km.



The solution, after the boundary values have been obtained as outlined above, is calculated in the same manner as in the preceding section 3.2.a.



#### 4. AN INVESTIGATION OF THE SOURCE EFFECTS IN SYMMETRIC AND NON-SYMMETRIC IONOSPHERIC CURRENT DISTRIBUTIONS

##### 4.1 The Symmetric Current Source Distribution

###### 4.1.a Mathematical Formulation of the Boundary Conditions

The coordinate system which is used throughout this section is given in Fig. 4.1. The conductor occupies the half-space  $z > 0$ , so that its boundary is the plane  $z = 0$ . The source current is assumed to flow parallel to the surface of the earth at height  $z = -|h|$  and is sinusoidally time dependent. The source current is symmetric about the line of maximum intensity.

In section 3.1.b it was shown that for a Gaussian source over a horizontally layered earth, the elementary electric field in the  $n$ th layer can be written

$$E_x^N = \{A_n \exp(-P \cdot z) + B_n \exp(P \cdot z)\} \cdot G(s) \cdot \cos(sy) \quad (4.1)$$

where  $(P)^2 = s^2 + i\omega\mu \cdot V_n$ .

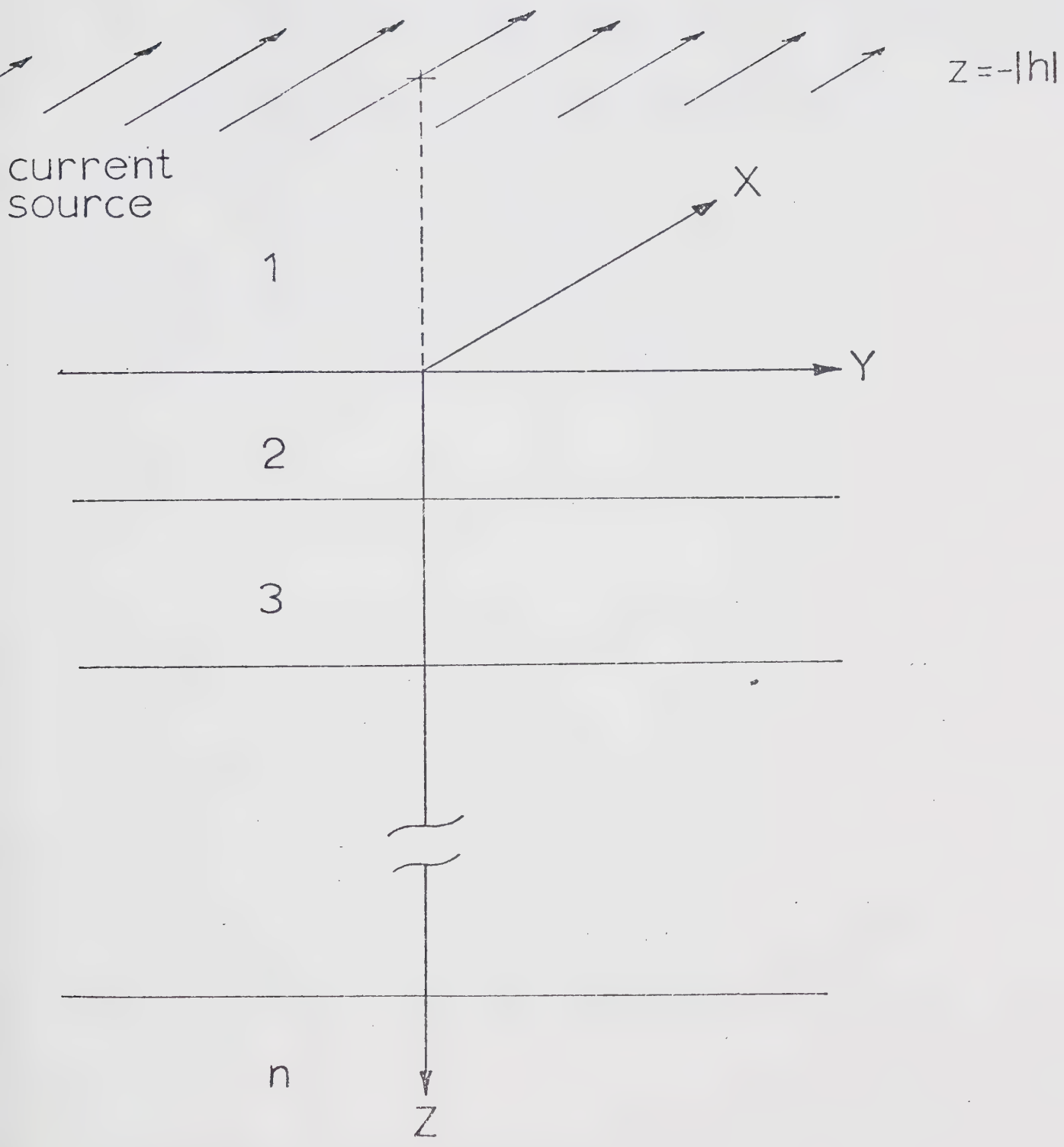
For a sheet current source with a Gaussian distribution function at height  $z = -|h|$  and a two-layered earth below, Peltier and Hermance (1971) show (as given in 3.23)







Fig. 4.1      The coordinate system, symmetric non-uniform  
source configuration and layered earth  
structure.





$$G(s) = -(iI \cdot wuk / \sqrt{2\pi} \cdot s) \cdot \exp(sz^0 - s^2 k^2 / 2). \quad (4.2)$$

where  $I \cdot$  is the maximum current intensity, and  $k$  is the standard deviation of the source.

To complete the solution,  $A_n$  and  $B_n$  must be determined and the eigenfunction for  $Ex^N$  given above must be summed over all values of  $s$  for each point where a value for the electric field is desired. That is

$$Ex(y, z) = \int_0^\infty \{A_n(P) \cdot \exp(-P \cdot z) + B_n(P) \cdot \exp(P \cdot z)\} \cdot G(s) \cdot \cos(sy) \, ds. \quad (4.3)$$

The half-space above the earth is taken as the first layer and if  $A_1 = 1$  then  $G(s)$  is a frequency dependent parameter of the source.  $B_1(P)$  is thought of as a reflection coefficient which represents the contribution to the total electric field above the earth from the subsurface layers. For a two-layered conductor  $B_2 = 0$  so that  $Ex^3$  will not become infinite with depth. The other  $A_n$  and  $B_n$  values can be obtained since the tangential components of  $Ex$  and  $Hy$  must be continuous across layer boundaries. This leads to

$$B_1 = \{(R-1)/(R+1)\} \quad (4.4)$$



where

$$R = s \cdot (Q+1) / [P_2 (Q-1)] \quad (4.5)$$

and

$$Q = \{(P_2 + P_3) / (P_2 - P_3)\} \cdot \exp(2 \cdot P_2 d) \quad (4.6)$$

which are identical to equations (3.11), (3.12) and (3.13), where  $d$  is the thickness of the first conducting layer. Also, we will have

$$A_2 = \{(1+B_1) \cdot Q\} / (Q+1), \quad (4.7)$$

$$B_2 = (1/Q) \cdot A_2, \quad (4.8)$$

$$A_3 = \{(A_2 + B_2 \cdot \exp(2 \cdot P_2 d)\} \cdot \exp[(P_3 - P_2) \cdot d]. \quad (4.9)$$

This general method of course may be extended to more layers. However, we will be concerned only with a two-layered earth.

#### 4.1.b Variation of $|E_x|$ , $|H_y|$ and $|H_z|$ due to a Non-Uniform Source above a Layered Conductor

To understand better the problem of induction by a non-uniform source, it is useful to study the variation





of the field component profiles with height and frequency over a layered earth. A two-layered earth has been considered with upper layer of resistivity 100 ohm-m and lower layer of resistivity 10 ohm-m. The current source with a Gaussian distribution in intensity and standard deviation of 240 km. which varies with periods of 10 sec,  $10^3$  sec and  $10^5$  sec is placed at height  $z = -|h| = -110$  km.

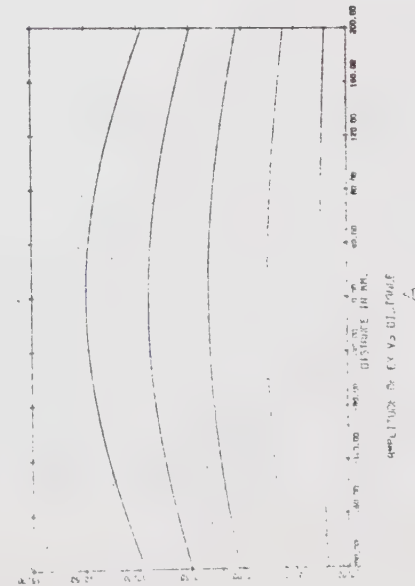
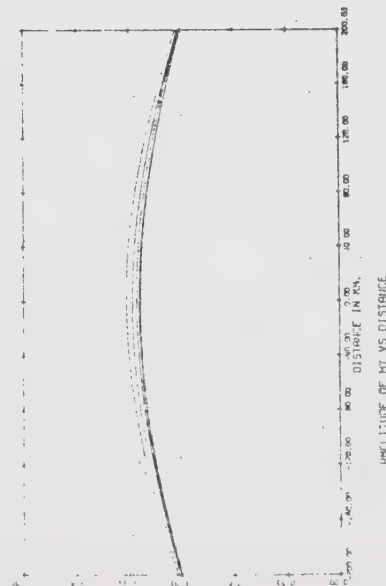
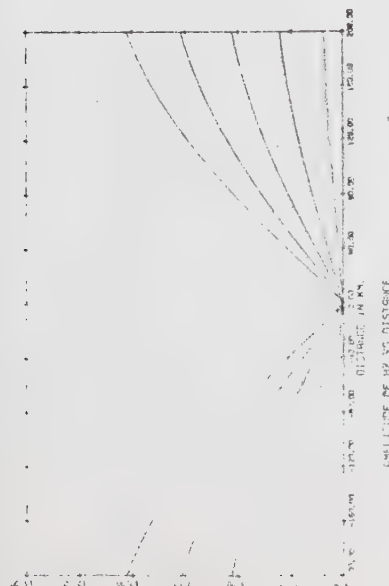
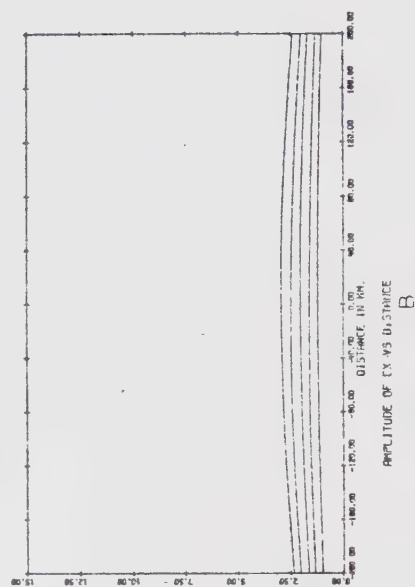
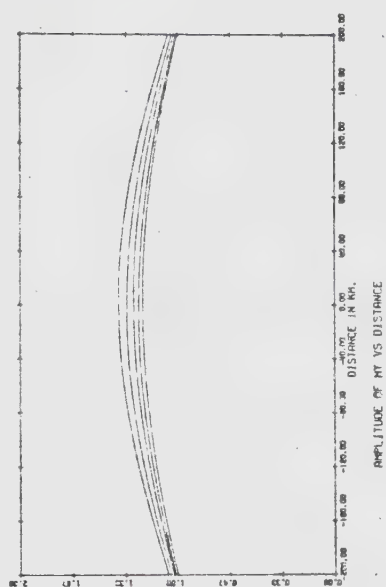
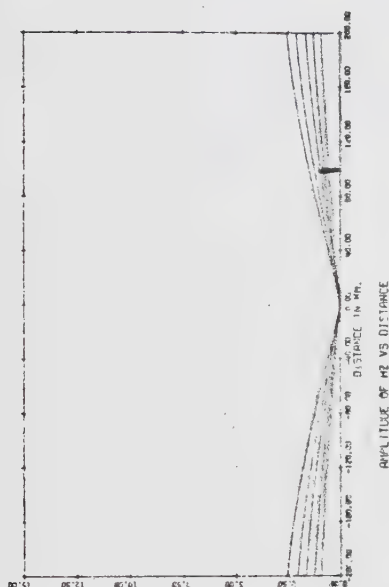
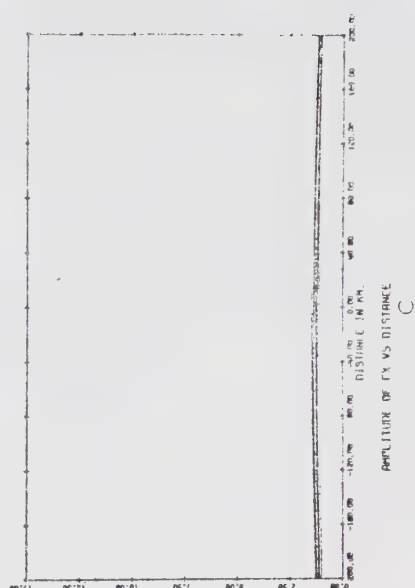
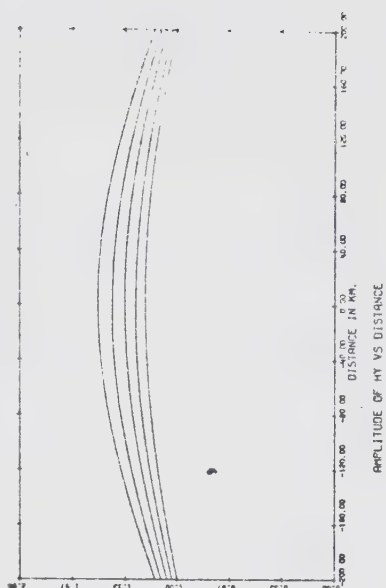
Fig. 4.2A shows the field profiles for the amplitudes of the three components  $E_x$ ,  $H_y$  and  $H_z$  for different heights above the surface of the conductor for ten seconds period. This figure clearly illustrates that above the surface of the conductor there is increasing uniformity of the field components as the surface is approached. That is, the source effect diminishes with increasing  $z$ . This uniformity of the field components near the surface is evident at all periods (Figs. 4.2B, 4.2C).

As the period increases, the field components become more uniform in the  $y$  direction, which reflects the change in the fundamental wave number of the field. Also, as the period increases, the skin depth in the conducting regions increases and the effect of the induced currents is to make the field more uniform.





Fig. 4.2       $|H_z|$ ,  $|H_y|$  and  $|E_x|$  profiles along the surface of the conductor and at heights of 25 km., 50 km., 75 km. and 100 km. above the conductor. (A) 10 sec. period, (B)  $10^3$  sec. period (C)  $10^5$  sec. period. All components are normalized with respect to a point on the surface of the conductor at 200 km. from the center of the source. For each component the bottom profile is the surface profile and the components increase in magnitude with height to the top profile at 100 km. above the surface.



I

I

B

C



The field component profiles conform well with Maxwell's equations. Referring to Fig. 4.2A, the spacing between the curves of  $|E_x|$ , which are calculated for different heights at equal intervals above the conductor and so are a measure of  $\partial|E_x|/\partial z$ , increases with decreasing  $z$ . Correspondingly,  $|H_y|$  increases with height. The spacing between the  $|E_x|$  curves depends on the horizontal distance of the field point from the center of the source. The maximum spacing occurs directly under the source (at 0.0 km.) and the minimum spacing occurs at  $\pm 200$  km.  $|H_y|$  will then decrease toward  $\pm 200$  km.  $\partial|E_x|/\partial y$  steadily increases from a minimum directly under the center of the source to maxima at  $\pm 200$  km., and so  $|H_z|$  increases from a minimum of zero under the center of the source to maxima at  $\pm 200$  km.

It is evident that the field distribution does not closely resemble the spatial distribution of the current source. The induction effects in the earth are principally responsible for this. Price (1965) has placed approximate limits on the source field dimensions. He estimates that the spatial wavelength of natural fields will be from approximately 400 km. to 40,000 km. Since the field distribution does not closely follow the spatial distribution of the source, this implies that even for





rather narrow current sources the spatial wavelength of the field still remains within the limits set by Price. This is evident from Fig. 4.3 where it is shown that for current distributions of different widths the electric field distribution at  $z=-100$  km. deviates further from a Gaussian curve as the source becomes narrower. Also, as the period increases the field tends to become more uniform. This trend is illustrated in the figure for periods of 10 sec. and 1000 sec., and it becomes more pronounced for longer periods.

It is the difference between the field distribution and the spatial distribution of the current that makes it imperative to compute the distribution of the field due to a particular non-uniform current source over an appropriately layered subsurface, and to obtain from such a calculation the boundary values for insertion into a model with lateral discontinuities.

#### 4.1.c The Solution for a Laterally Inhomogeneous Structure and Apparent Resistivity Curves.

After the application of the above method to obtain the boundary values for the finite difference method, solutions were obtained for a two-dimensional model with a lateral inhomogeneity as illustrated in





Fig. 4.3      E-field profiles at  $z=-100$  km. for current sources of standard deviation 240 km., 120 km. and 60 km. for 10 sec. and 1000 sec. period compared with corresponding Gaussian curves. Normalized with respect to the point under the center of the source.

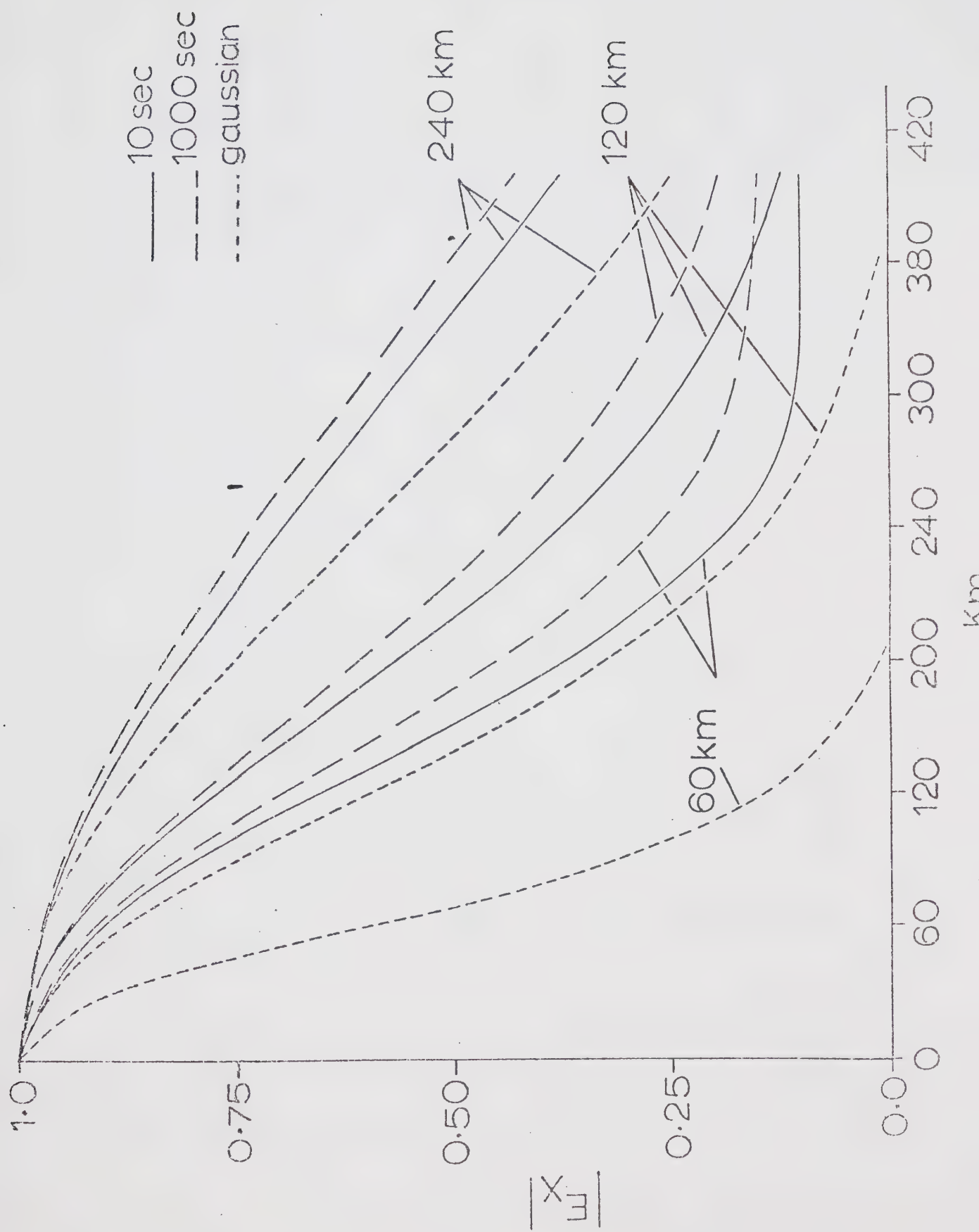




Fig. 4.4. The position of the source with respect to the inhomogeneous structure is shown in Fig. 4.5. The source is located at  $z = -110$  km. and is displaced relative to the center of the inhomogeneity by 720 km. The standard deviation of the source is 240 km, and so the center of the inhomogeneity is 3 standard deviations from the center of the source. The field distributions due to the non-uniform source over a multiple layered earth without the inhomogeneity were calculated at positions corresponding to the boundary of the mesh as illustrated in Fig. 4.4. These were then inserted into the iterative finite difference program and solutions obtained.

Apparent resistivity curves for different positions under the Gaussian source over the layered earth without any inhomogeneity are shown in Fig. 4.6 and are compared with the apparent resistivity curve for a uniform source. It can be seen that at long periods the apparent resistivity curves spread away from the uniform source curve. This effect was observed by Peltier and Hermance (1971) for their models.

In Fig. 4.7 are given the apparent resistivity curves calculated from the Cagniard (1953) formula for the conductivity structure shown in Fig. 4.4 for







Fig. 4.4      Conductivity configuration for the lateral discontinuity model. H-values; horizontal grid sizes in km.; K-values; vertical grid sizes in km. Sigma represents the conductivity in e. m. u., so that for region B, resistivity=0.25 ohm-m; region C, resistivity=250 ohm-m.



Fig. 4.5      Source location relative to the inhomogeneous  
structure. Distances in km. (Not to scale).

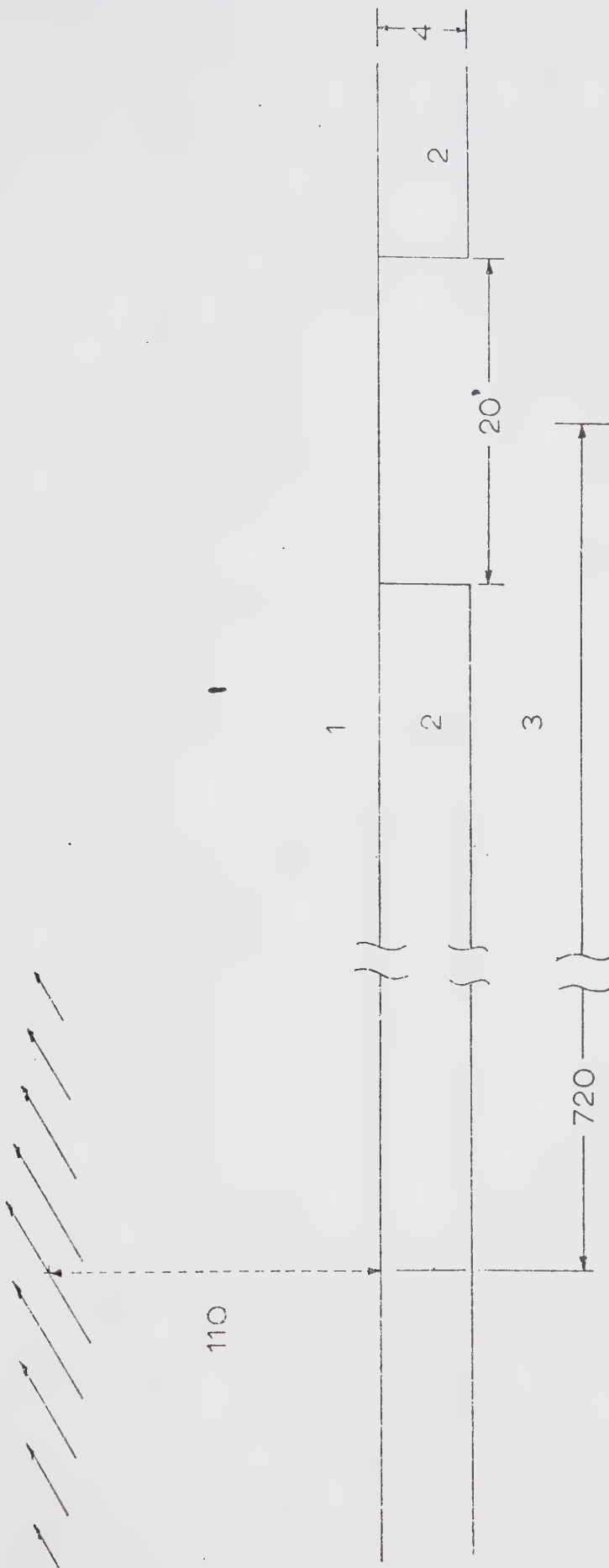








Fig. 4.6      Apparent resistivity curves for Gaussian source over layered earth compared with uniform source. The curves are for different positions under the source, 0=directly under, 0.5=one-half a standard deviation from the center etc.

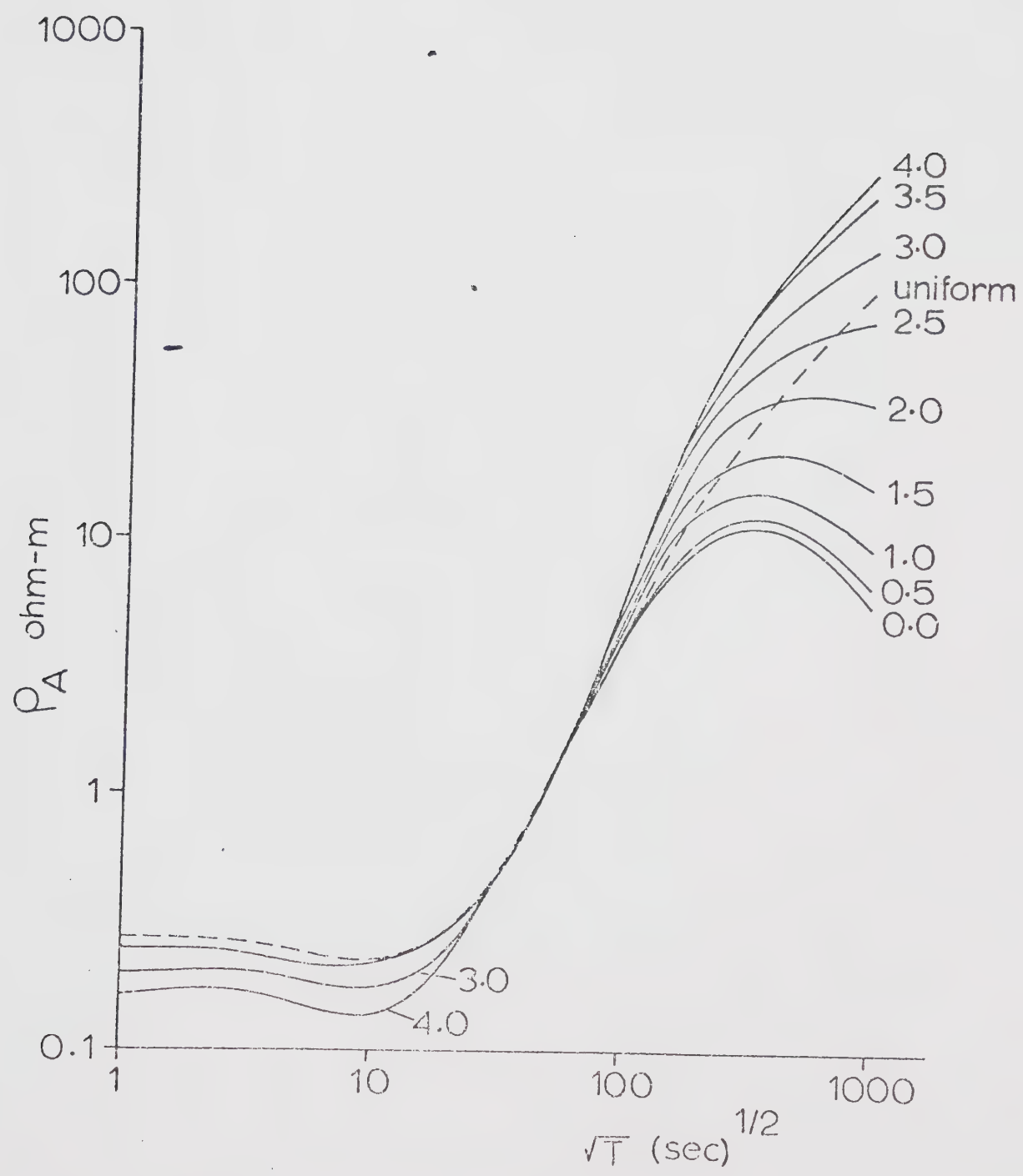
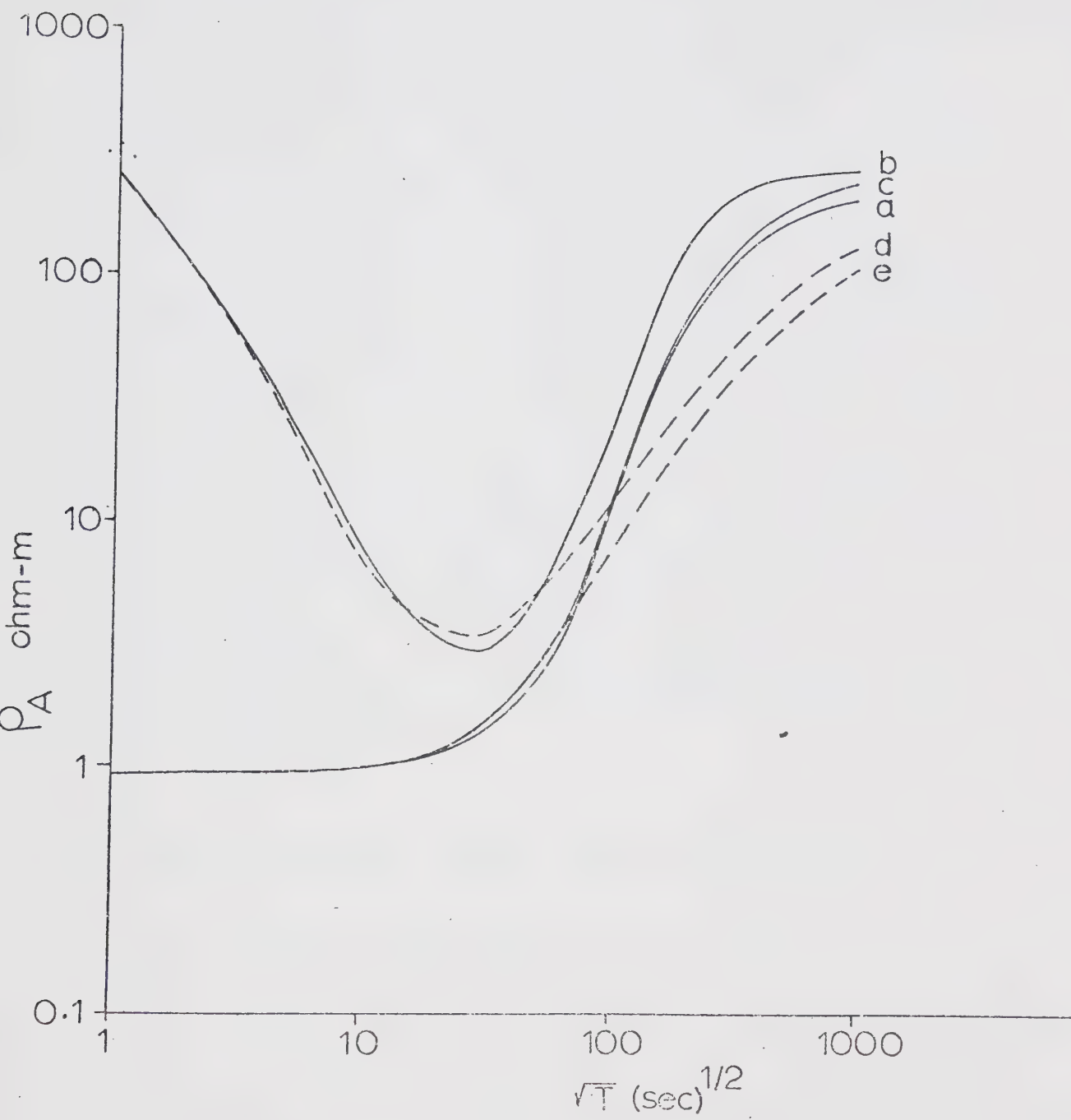






Fig. 4.7      Apparent resistivity curves for different positions over the lateral inhomogeneity.

- (a) left edge of inhomogeneity, Gaussian source.
- (b) center of inhomogeneity, Gaussian source.
- (c) right edge of inhomogeneity, Gaussian source.
- (d) center of inhomogeneity, uniform source.
- (e) edges of inhomogeneity, uniform source.





three different positions above the inhomogeneity for both Gaussian and uniform sources. At shorter periods the apparent resistivity varies widely with position for the Gaussian source. The apparent resistivity calculation at the center of the inhomogeneity tends to approach the value of the higher resistivity material. At the edges of the inhomogeneity the calculations of apparent resistivity give values more closely related to the resistivity of the lower resistivity material. For longer periods the non-symmetry of the inducing field above the inhomogeneity causes a spreading of the resistivity curves at the edges of the inhomogeneity. Apparent resistivity curves for the uniform source, as in the layered case, follow the non-uniform source curves at short periods but deviate from them at longer periods.

## 4.2 The Non-Symmetric Current Source Distribution

### 4.2.a Mathematical Formulation of the Boundary Conditions

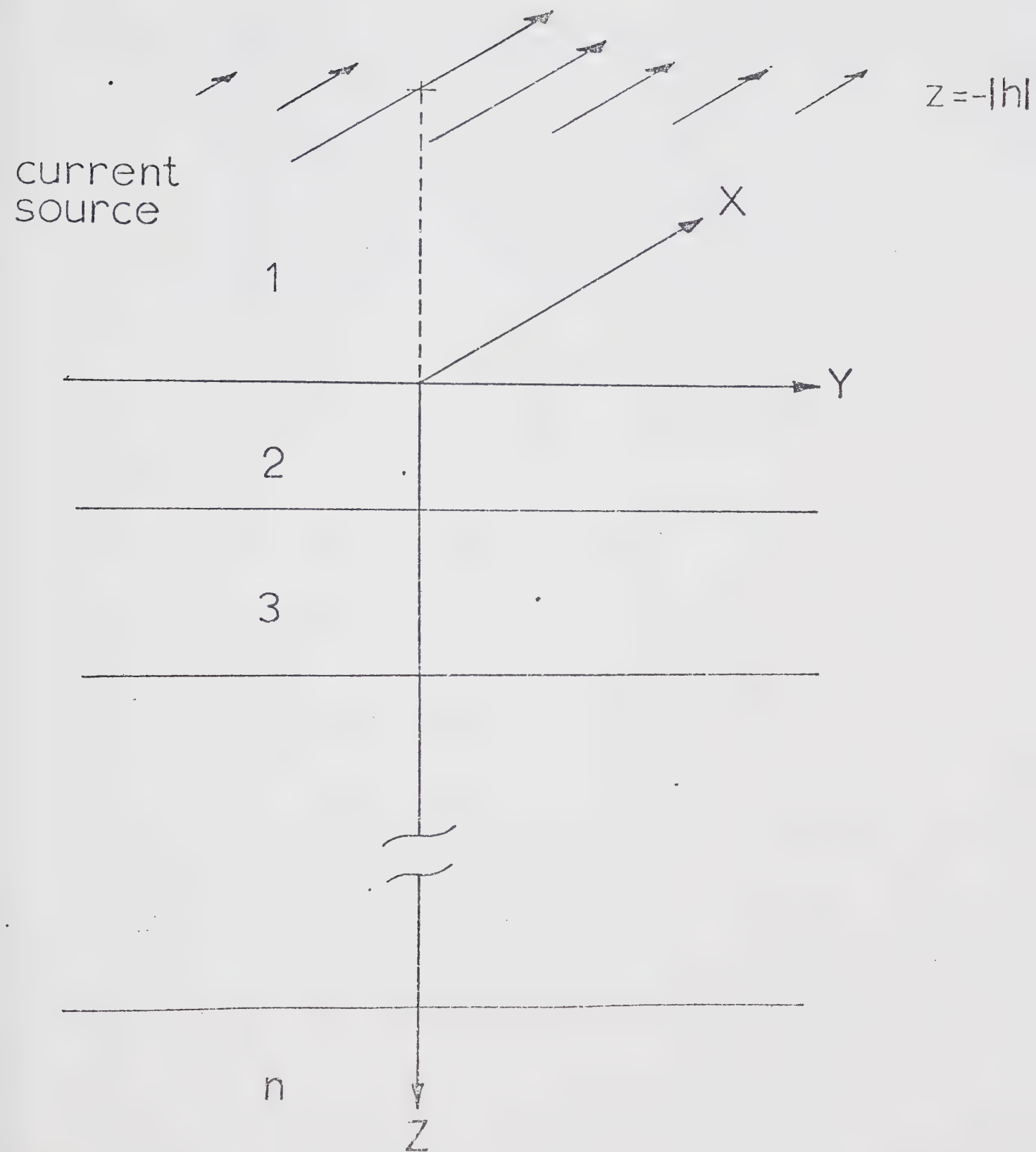
Illustrated in Fig 4.8 is the coordinate system which will be used throughout this derivation. The source is a sheet of current which flows parallel to the surface of the earth at height  $z=-|h|$ , is sinusoidally time dependent and is non-symmetric in spatial distribution







Fig. 4.8      The coordinate system, non-symmetric source  
intensity distribution and layered earth  
structure.





with the general intensity distribution of the form  $y \cdot \exp(py)$ .

In the two-dimensional E-polarization problem with the period sufficiently long so that displacement currents may be neglected, Maxwell's equations reduce to the diffusion equation as given previously in (1.9).

By a separation of variables, solutions of the form  $E_x(y, z) = Y(y) \cdot Z(z)$  are obtained. For a horizontally layered earth

$$Y(y) = C(s, y^0) \cdot \cos(sy) + D(s, y^0) \cdot \sin(sy), \quad (4.10)$$

and

$$Z(z) = A_n(P) \cdot \exp(-P \cdot z) + B_n(P) \cdot \exp(P \cdot z) \quad (4.11)$$

where  $(P)^2 = s^2 + i\omega\mu \cdot V_n$ , and  $s$ ,  $y^0$  and  $V_n$  are the spatial wave number, current line source position and the homogeneous conductivity of the  $n$ th layer respectively.

The elementary electric field in the  $n$ th layer can be written as

$$E_x(y, z) = \{A_n(P) \cdot \exp(-P \cdot z) + B_n(P) \cdot \exp(P \cdot z)\}$$



$$\cdot \{C(s, y^0) \cdot \cos(sy) + D(s, y^0) \cdot \sin(sy)\}. \quad (4.12)$$

The elementary magnetic field components  $H_y(y, z)$  and  $H_z(y, z)$  are obtained by taking the curl of (4.12).

$$\begin{aligned} H_y(y, z) = & -(i/wu) \cdot P \{A_n(P) \cdot \exp(-P \cdot z) - B_n(P) \\ & \cdot \exp(P \cdot z)\} \cdot \{C(s, y^0) \cdot \cos(sy) \\ & + D(s, y^0) \cdot \sin(sy)\} \end{aligned} \quad (4.13)$$

$$\begin{aligned} H_z(y, z) = & +(i/wu) \cdot s \{A_n(P) \cdot \exp(-P \cdot z) + B_n(P) \\ & \cdot \exp(P \cdot z)\} \cdot \{C(s, y^0) \cdot \sin(sy) \\ & - D(s, y^0) \cdot \cos(sy)\}. \end{aligned} \quad (4.14)$$

If the half space above the earth is defined as the first layer,  $V_1=0$ ,  $P_1=s$ , and  $A_1(P)=1$ , then  $C(s, y^0)$  and  $D(s, y^0)$  are parameters which characterize the source and are dependent upon the frequency and source position.

The solution for a current source which has a general non-uniform spatial distribution can be obtained from the superposition of suitably weighted line current source solutions. In order to accomplish this, the constants  $C(s, y^0)$  and  $D(s, y^0)$  in (4.12) must be calculated for a line source. Assuming that the conductivity of the whole earth is zero, then  $B_1=0$  and the horizontal component of the magnetic field  $H_y^1$  would be





given by Ampere's law for a line current source:

$$H_y^1 = -(I_0/2\pi) \cdot (z-z^0) / \{(z-z^0)^2 + (y-y^0)^2\} \quad (4.15)$$

where  $z^0 = -|h|$  and  $y^0$  is the horizontal position of the line current source. From (4.13) with  $V_1=0$ ,  $B_1=0$  and  $P_1=s$ , the general solution for  $H_y$  is obtained by summing all possible solutions of type (4.15) over the allowable range of  $s$  ( $0 < s < \infty$ ):

$$\begin{aligned} H_y^1 = & -(i/wu) \cdot \int_0^\infty s \cdot \{\exp(-sz)\} \cdot \{C(s, y^0) \cdot \cos(sy) \\ & + D(s, y^0) \cdot \sin(sy)\} ds = -(I_0/2\pi) \\ & \cdot (z-z^0) / \{(z-z^0)^2 + (y-y^0)^2\}. \end{aligned} \quad (4.16)$$

Using the inverse Laplace transforms,

$$\begin{aligned} (z-z^0) / \{(z-z^0)^2 + (y-y^0)^2\} &= \int_0^\infty \exp(-sz) \cdot \exp(z^0 s) \\ &\cdot \cos([y-y^0] \cdot s) ds = \int_0^\infty \exp(-zs) \cdot \exp(z^0 s) \\ &\cdot \{\cos(sy^0) \cdot \cos(sy) + \sin(sy^0) \cdot \sin(sy)\} ds, \end{aligned} \quad (4.17)$$

the integral equation for  $C(s, y^0)$  and  $D(s, y^0)$  can be solved if we set

$$C(s, y^0) = C'(s) \cdot \cos(sy^0) \quad (4.18)$$



and

$$D(s, y^0) = C'(s) \cdot \sin(sy^0) \quad (4.19)$$

where

$$C'(s) = -(i\omega I_0 / 2\pi s) \cdot \exp(z^0 s). \quad (4.20)$$

For the non-symmetric current intensity distribution

$$I_x(y^0) = I_0 \cdot (y^0 - b) \cdot \exp\{-a(y^0 - b)\} \cdot u(y^0 - b) \quad (4.21)$$

where  $I_0$ ,  $b$  and  $a$  are constants and  $u(y^0 - b)$  is the unit step function, we assume that the source is a composite of elemental line sources having intensities described by (4.21). The magnetic field intensity that such a source at  $(y^0, z^0)$  contributes to the observed total field at  $(y, z)$  is

$$\begin{aligned} H_{x1}(\text{element}) = & -(I_0 / 2\pi) \cdot (y^0 - b) \cdot \exp\{-a(y^0 - b)\} \\ & \cdot \{(z - z^0) / [(z - z^0)^2 + (y - y^0)^2]\} \cdot u(y^0 - b). \end{aligned} \quad (4.22)$$

The total magnetic field  $H_{x1}(y, z)$  can be obtained by



integrating over all  $y^0$  ( $b < y^0 < \infty$ );

$$Hx^1(y, z) = -(I \bullet / 2\pi) \cdot \int_c^\infty (y^0 - b) \cdot \exp\{-a(y^0 - b)\} \cdot \{(z - z^0) / [(z - z^0)^2 + (y - y^0)^2]\} dy^0. \quad (4.23)$$

As before,

$$Hx^1(y, z) = -(i/wu) \cdot \int_0^\infty s \cdot \exp(-sz) \cdot \{V(s) \cdot \cos(sy) + W(s) \cdot \sin(sy)\} ds \quad (4.24)$$

where  $V(s)$  and  $W(s)$  are source constants which can be obtained in the same manner as  $C(s, y^0)$  and  $D(s, y^0)$ . The source constants will not be a function of  $y^0$  (source position) since this is the variable over which the integration has been taken in (4.24). Equating (4.23) and (4.24), we have

$$-(i/wu) \cdot \int_0^\infty s \cdot \exp(-sz) \cdot \{V(s) \cdot \cos(sy) + W(s) \cdot \sin(sy)\} ds = -(I \bullet / 2\pi) \cdot \int_0^\infty (y^0 - b) \cdot \exp\{-a(y^0 - b)\} \cdot \{(z - z^0) / [(z - z^0)^2 + (y - y^0)^2]\} dy^0. \quad (4.25)$$

If in (4.16) both sides are multiplied by  $(y^0 - b) \cdot \exp\{-a(y^0 - b)\}$  and then integrated over all  $y^0$  we have;

$$-(i/wu) \cdot \int_b^\infty \int_0^\infty s \cdot \exp(-sz) \cdot (y^0 - b) \cdot \exp\{-a(y^0 - b)\}$$



$$\begin{aligned}
& \cdot \{C(s, y^0) \cdot \cos(sy) + D(s, y^0) \cdot \sin(sy)\} \, ds \, dy^0 \\
= & -(I \bullet / 2\pi) \cdot \int_b^\infty (y^0 - b) \cdot \exp\{-a(y^0 - b)\} \cdot \{(z - z^0) \\
& / [(z - z^0)^2 + (y - y^0)^2]\} \, dy^0.
\end{aligned} \tag{4.26}$$

Comparing (4.25) and (4.26) and solving for  $V(s)$  and  $W(s)$  gives

$$\begin{aligned}
V(s) = & -(iwuI \bullet \cdot \exp(sz^0) / 2\pi s) \cdot \{[(a^2 - s^2) \cdot \cos(sb) \\
& - 2as \cdot \sin(sb)] / (a^2 + b^2)^2\}
\end{aligned} \tag{4.27}$$

and

$$\begin{aligned}
W(s) = & -(iwuI \bullet \cdot \exp(sz^0) / 2\pi s) \cdot \{[2as \cdot \cos(sb) \\
& + (a^2 - s^2) \cdot \sin(sb)] / (a^2 + s^2)^2\}.
\end{aligned} \tag{4.28}$$

Summing over all values of  $s$ , the electric field in the  $n$ th layer is

$$\begin{aligned}
Ex^N(y, z) = & \int_0^\infty \{An(P) \cdot \exp(-P \cdot z) + Bn(P) \cdot \exp(P \cdot z)\} \\
& \cdot \{V(s) \cdot \cos(sy) + W(s) \cdot \sin(sy)\} \, ds.
\end{aligned} \tag{4.29}$$

The magnetic field components are

$$Hy^N(y, z) = -(i/wu) \cdot \int_0^\infty P \{An(P) \cdot \exp(-P \cdot z) - Bn(P)$$





$$\cdot \exp(P.z) \} \cdot \{V(s) \cdot \cos(sy) + W(s) \cdot \sin(sy)\} ds \quad (4.30)$$

$$H_z^N(y,z) = +(i/wu) \cdot \int_0^\infty s \{A_n(P) \cdot \exp(-P.z) + B_n(P) \cdot \exp(P.z)\} \cdot \{V(s) \cdot \sin(sy) - W(s) \cdot \cos(sy)\} ds. \quad (4.31)$$

Completion of the solution requires  $A_n(P)$  and  $B_n(P)$  to be found for each layer. The half space above the earth is taken as the first layer, and if  $A_1(P)=1$  then  $V(s)$  and  $W(s)$  are frequency dependent parameters of the source. These quantities have been previously given in section 4.1.a.

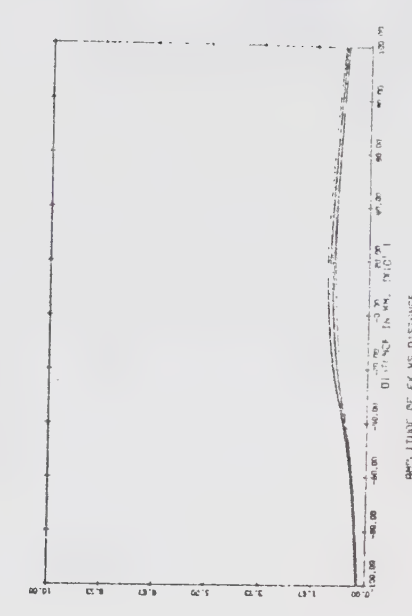
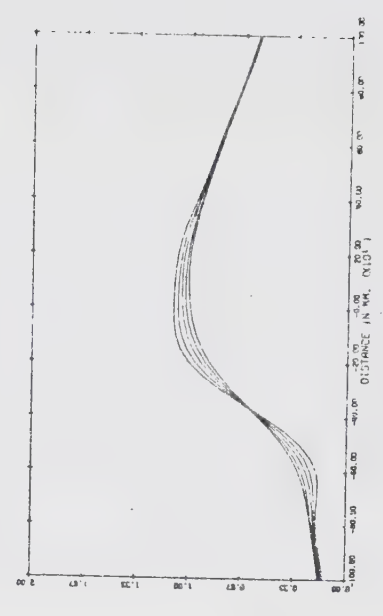
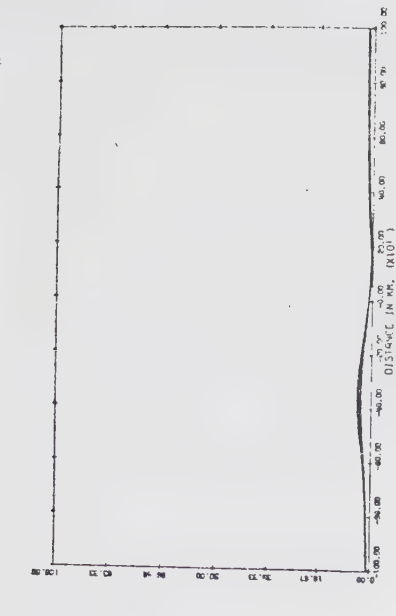
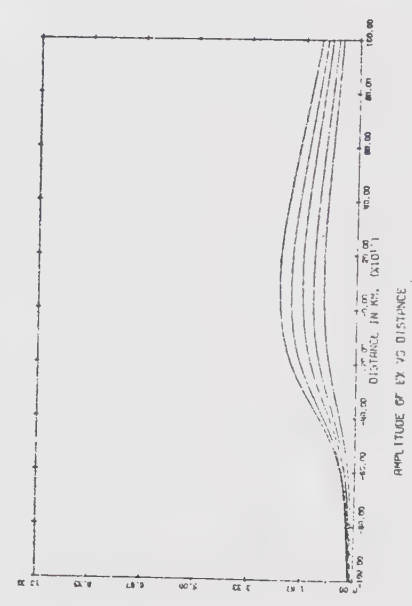
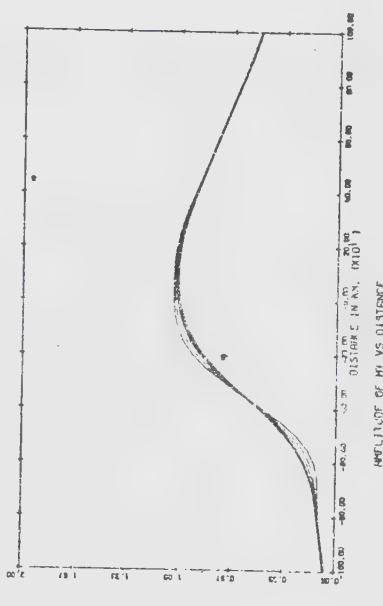
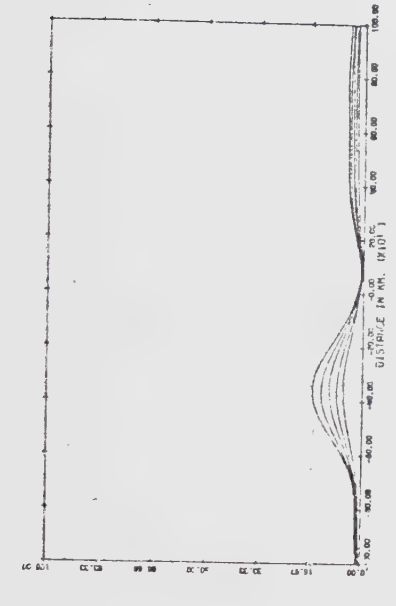
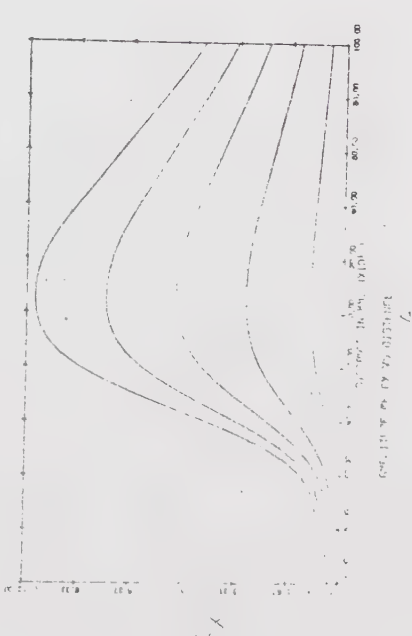
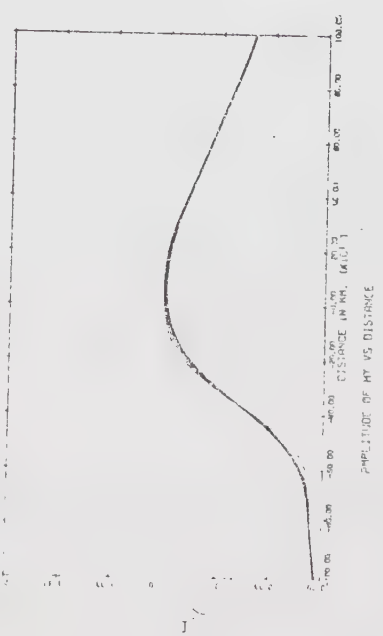
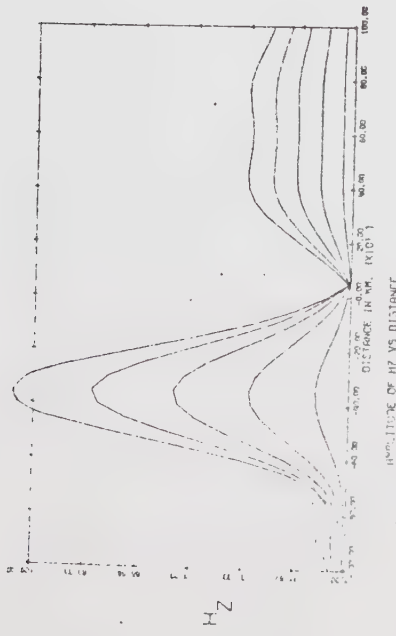
#### 4.2.b Variation of $|E_x|$ , $|H_y|$ and $|H_z|$ due to a Non-Symmetric Source and Apparent Resistivity Curves.

It is interesting to compare the field component profiles with height and frequency over a layered earth, and examples are shown in Fig. 4.9. A two-layered earth with the thickness of the upper layer equal to 50 km. and resistivity of 100 ohm-m and lower layer of resistivity 10 ohm-m has been considered. The non-symmetric current source has an intensity distribution of  $(y-b) \cdot \exp\{(-1/|b|) \cdot (y-b)\}$  with  $b=-480$  km., and is placed at a height of  $z=-|h|=-110$  km. The field component profiles for





Fig. 4.9       $|H_z|$ ,  $|H_y|$  and  $|E_x|$  profiles along the surface of the conductor and at heights of 25 km., 50 km., 75 km. and 100 km. above the conductor. (A) 10 sec. period, (B)  $10^3$  sec. period (C)  $10^5$  sec. period. All components are normalized with respect to a point on the surface at the origin.



B



periods of 10 sec.,  $10^3$  sec. and  $10^5$  sec. are shown in A, B and C of Fig. 4.9 respectively. These figures display the amplitudes of the three components  $|H_z|$ ,  $|H_y|$  and  $|E_x|$  for different heights above the surface of the conductor. The maximum amplitude in each case is for the maximum height, with amplitude decreasing as the surface is approached.

The non-symmetric current distribution of the source is clearly reflected in the field component profiles. The field components differ greatly for positive and negative  $y$ , decreasing rapidly in the region of negative  $y$  above which the source intensity is zero. While the fields are in general non-uniform there are similarities to the field components of the symmetric Gaussian source given in section 4.1.b. The fields become increasingly uniform as the surface is approached. This effect is evident at all periods. The source effect therefore diminishes with increasing  $z$  just as in the Gaussian source case. As the period increases the field components become more uniform in the  $y$  direction, which reflects the change in the fundamental wave number of the field. This effect was also noted in the Gaussian source case.

Apparent resistivity curves are shown in





Fig. 4.10 for various positions under the source on the surface of the conductor. Fig. 4.10A and Fig. 4.10B show the apparent resistivity curves in the negative and positive  $y$  regions respectively at intervals of 200 km. to a maxima of  $\pm 1000$  km. The curves of Fig. 4.10B resemble the Gaussian source curves (see Fig. 2, Peltier and Hermance, 1971). However, the curves of Fig 4.10A contrast sharply at longer periods. This effect can be attributed to the discontinuity of the current source in the negative  $y$  region.

#### 4.2.c The Solution for a Laterally Inhomogeneous Structure and Apparent Resistivity Curves.

After the application of the above method to obtain the boundary values for the finite difference method, solutions were obtained for a two-dimensional model with a lateral inhomogeneity as illustrated in Fig. 4.11. The position of the source with respect to the inhomogeneous structure is shown in Fig. 4.12. The source is located at  $z=-110$  km. and is displaced relative to the center of the inhomogeneity by  $\pm 920$  km. The intensity distribution of the source remains the same as described in section 4.2.b.





Fig. 4.10      Apparent resistivity curves for  $y \cdot \exp(py)$  source over layered earth compared with uniform source (dashed curve), A-negative y region, B-positive y region,  $V_1 = 100$  ohm-m;  $V_2 = 10$  ohm-m.

- (a) at origin
- (b) 200 km. from origin
- (c) 400 km. from origin
- (d) 600 km. from origin
- (e) 800 km. from origin
- (f) 1000 km. from origin

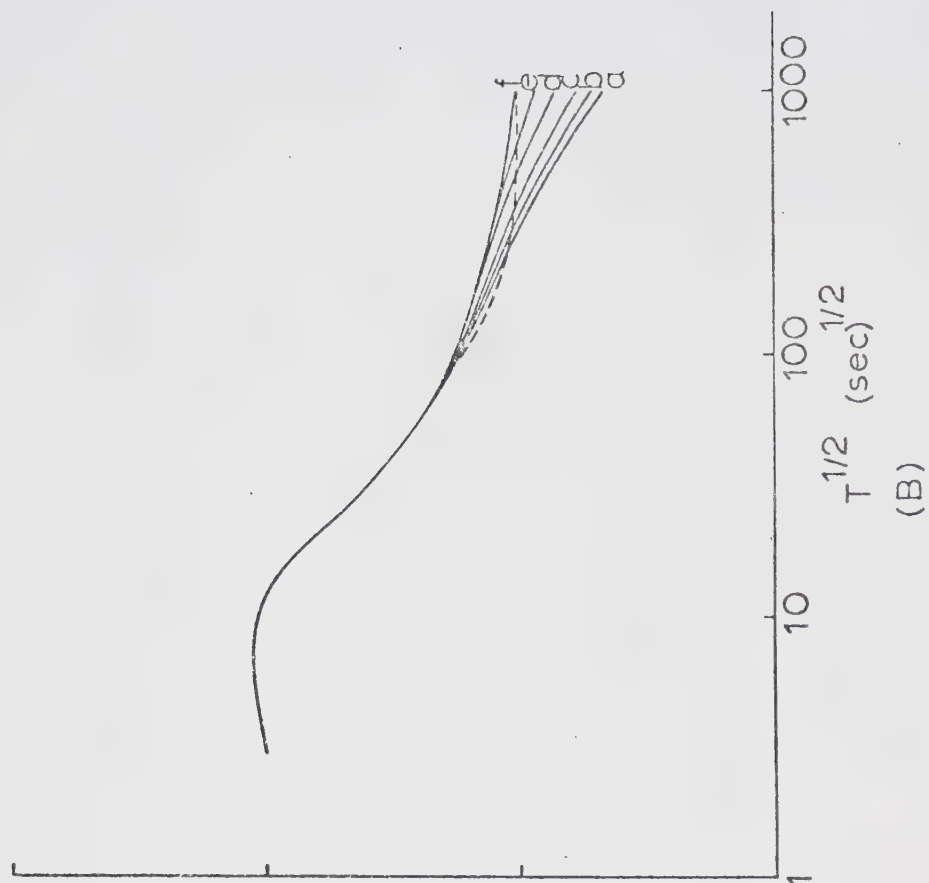
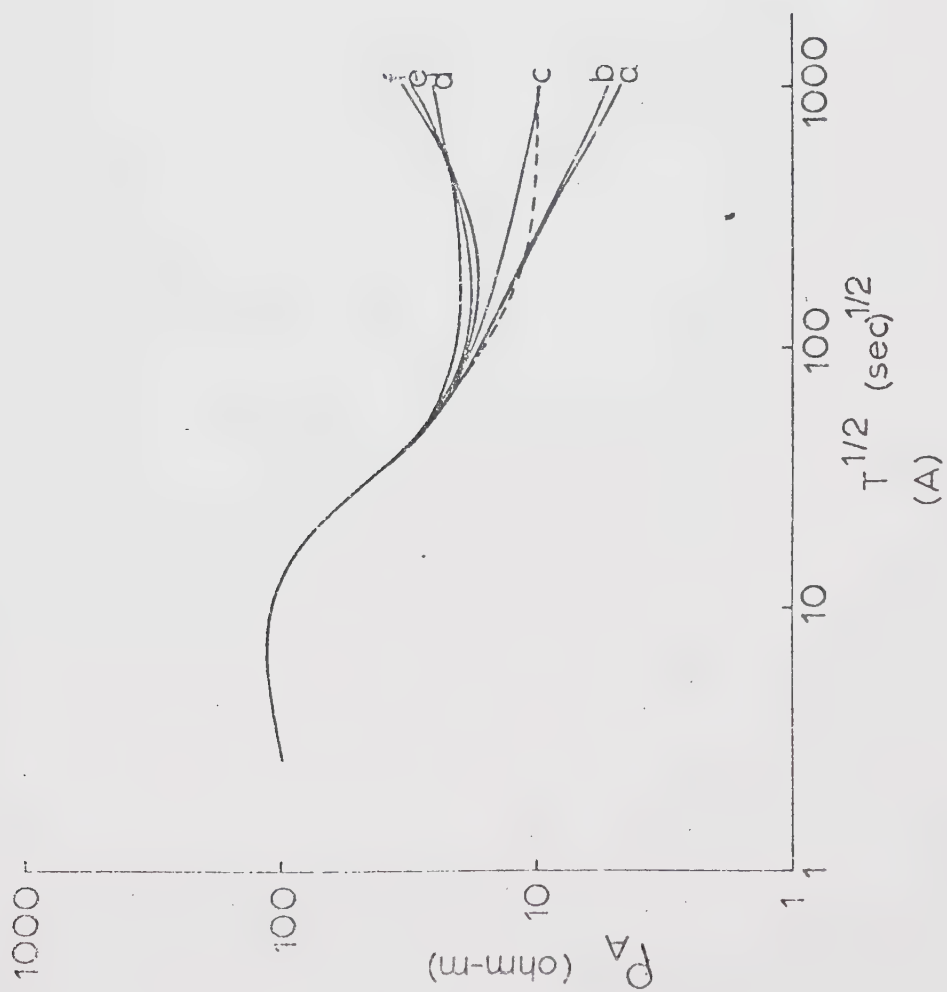








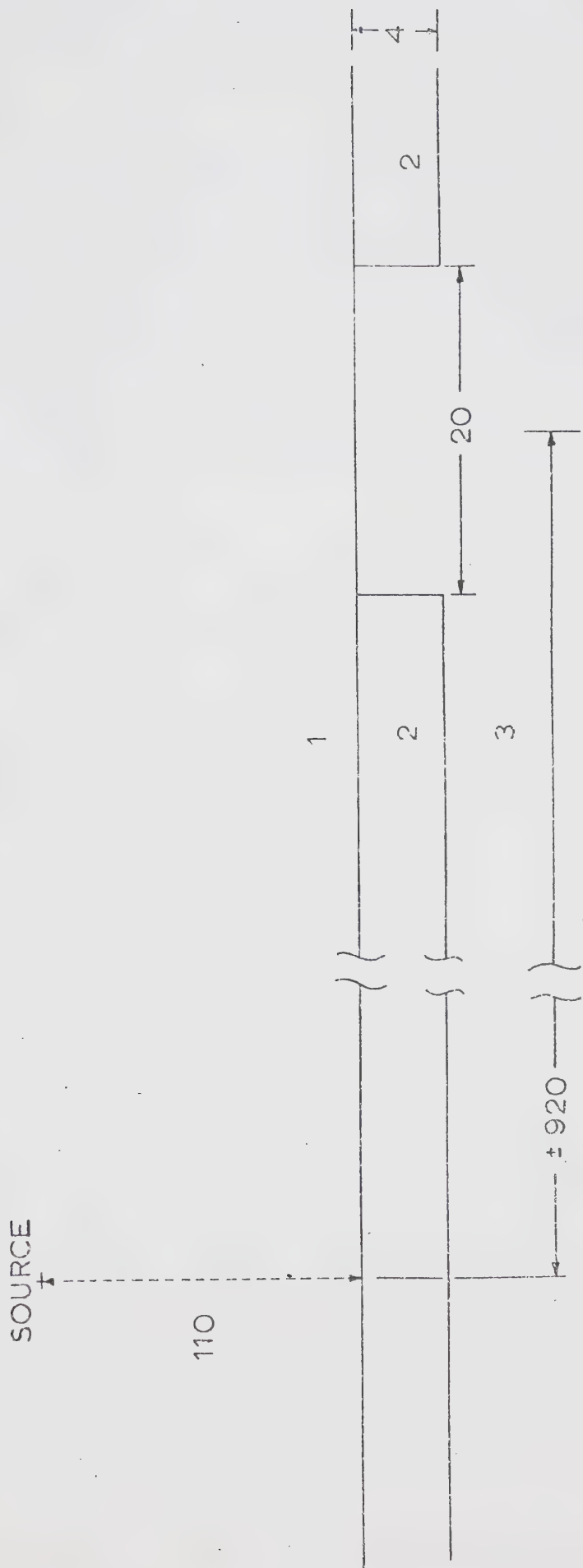
Fig. 4.11      Conductivity configuration for the lateral discontinuity model. H-values; horizontal grid sizes in km.; K-values; vertical grid sizes in km. Sigma represents the conductivity in e. m. u., so that for region E, resistivity=0.25 ohm-m; region C, resistivity=250 ohm-m.







Fig. 4.12      Source location relative to the inhomogeneous structure. Distances in km. (Not to scale).





Apparent resistivity curves for different positions under the source over the layered earth without any inhomogeneity are shown in Figs. 4.13A and 4.13B. Again at long periods the apparent resistivity curves spread away from the uniform source curve, and Figs. 4.13A and 4.13B differ due to source asymmetry.

Fig. 4.14 gives the apparent resistivity curves for the conductivity structure shown in Fig. 4.11 for three different positions above the inhomogeneity for non-symmetric and uniform sources. Parts A and B of this figure refer to regions  $y < 0$  and  $y > 0$  respectively. As in the Gaussian source case, for shorter periods the apparent resistivity varies widely with position. The apparent resistivity value at the center of the inhomogeneity tends to approach the value of the higher resistivity material. At the edges of the inhomogeneity the calculation of apparent resistivity gives values more closely related to the resistivity of the lower resistivity material. For longer periods the non-symmetry of the inducing field above the inhomogeneity causes a spreading of the resistivity curves at the edges of the inhomogeneity. These general trends hold true for both parts A and B. As before the positive and negative  $y$  region curves differ substantially. As in the layered case, the apparent







Fig. 4.13      Apparent resistivity curves for the  $y \cdot \exp(py)$  source over layered earth without any inhomogeneity compared with uniform source (dashed curve). A-negative  $y$  region; B-positive  $y$  region,  $V_1 = .25$  ohm-m;  $V_2 = 250$  ohm-m.

- (a) at origin
- (b) 200 km. from origin
- (c) 400 km. from origin
- (d) 600 km. from origin
- (e) 800 km. from origin
- (f) 1000 km. from origin

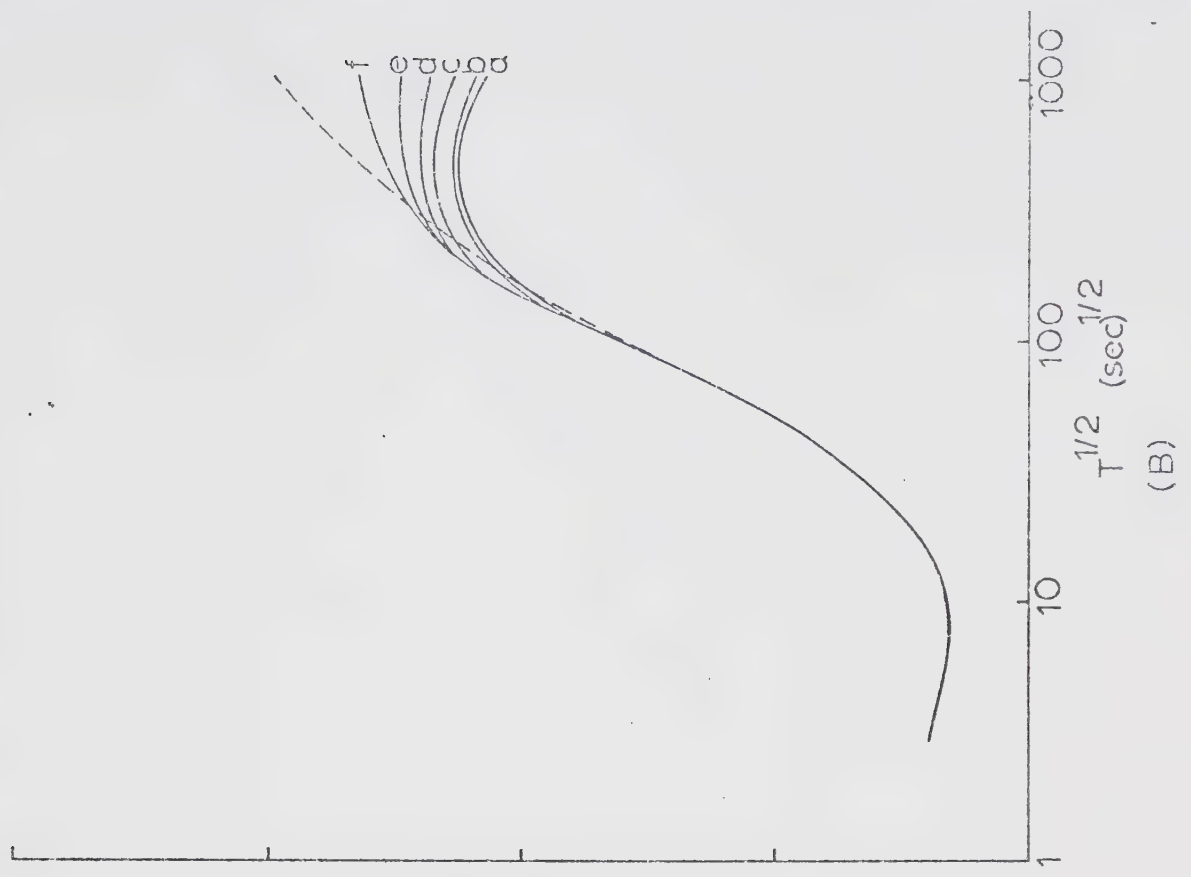
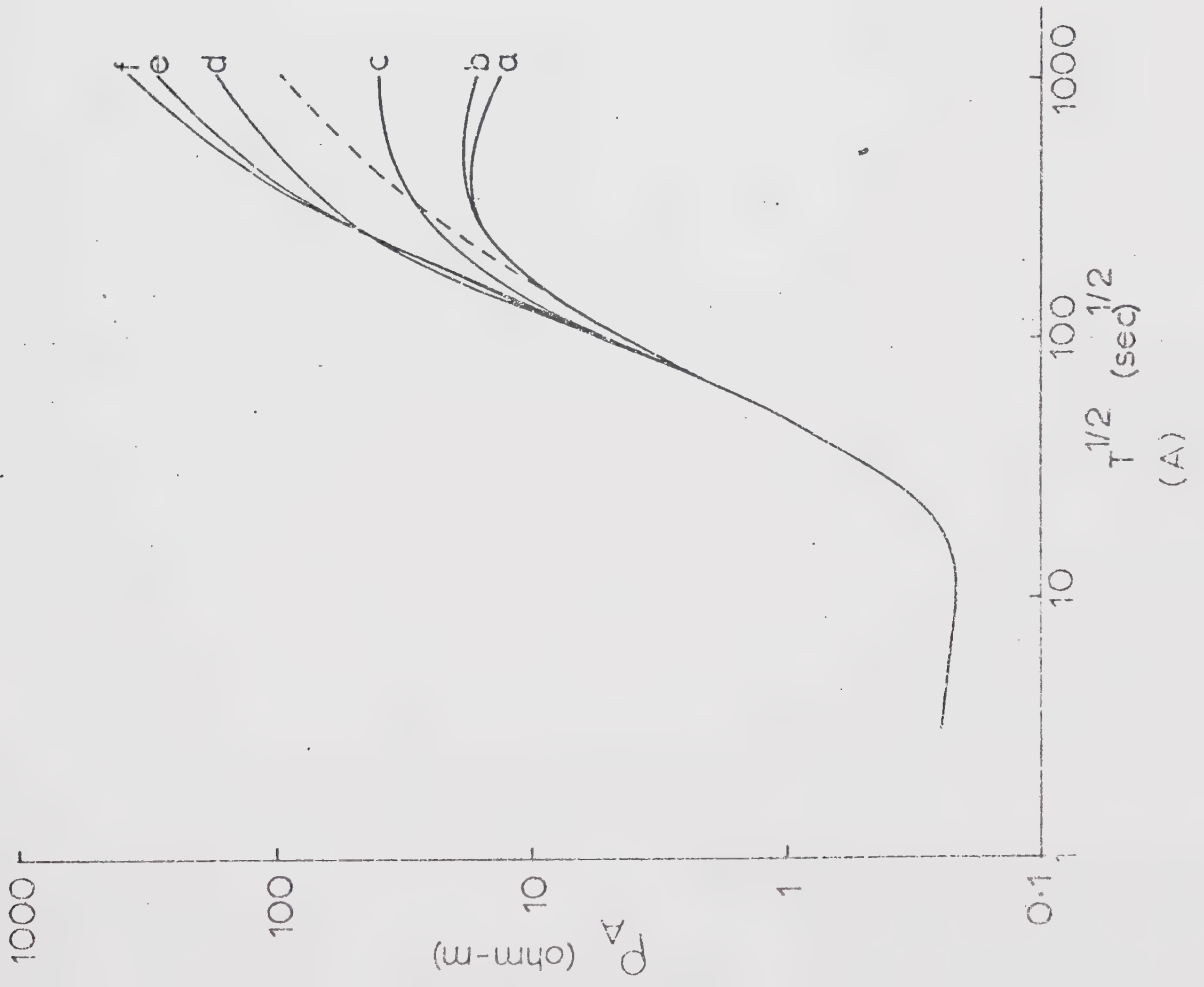






Fig. 4.14      Apparent resistivity curves for different positions over the lateral inhomogeneity. A-negative y region; B-positive y region.

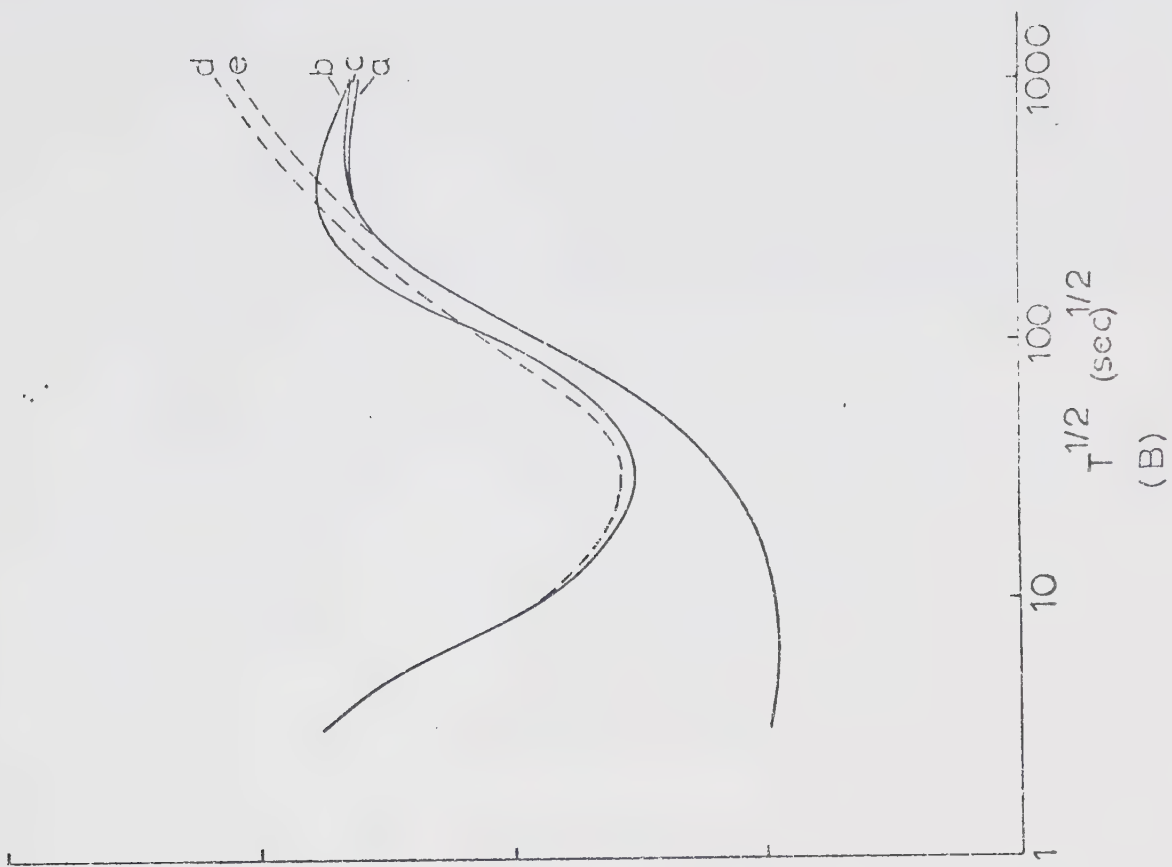
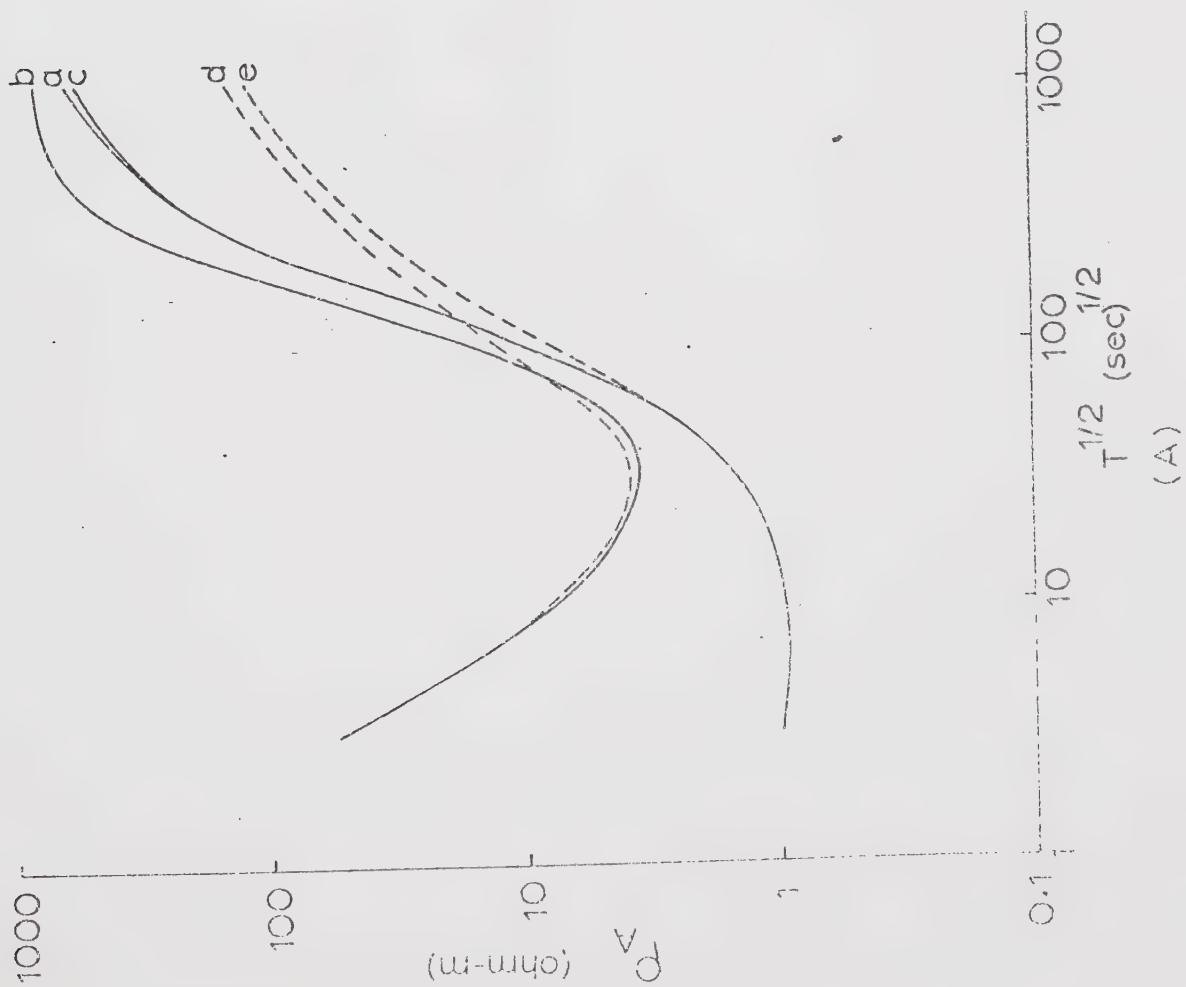
(a) left edge of inhomogeneity,  $y \cdot \exp(py)$  source.

(b) center of inhomogeneity,  $y \cdot \exp(py)$  source.

(c) right edge of inhomogeneity,  $y \cdot \exp(py)$  source.

(d) center of inhomogeneity, uniform source.

(e) edges of inhomogeneity, uniform source.







resistivity curves for the uniform source deviate from the curves of the non-symmetric source at longer periods.



## 5. ELECTROMAGNETIC INDUCTION IN THE EARTH BY AN APERIODIC NON-UNIFORM CURRENT SOURCE

### 5.1.a The Two-Dimensional Double Current System

Little attention has been given to the problem of electromagnetic induction by a non-uniform source which is temporally aperiodic and also exhibits spatial variation with time. Price (1950) examined aperiodic inducing fields and considered the effects due to a sudden increase in the inducing field and the solution for any other time variation could then be obtained. The special case of a stationary line current parallel to the surface of the earth in which a sudden increase in the line current intensity took place was considered by him. Also, Wait (1954) considered the transient response of the tangential electric field for a unit step increase in the magnetic field. The calculations by Wait (1954) which are applicable to non-uniform sources, were made for subsurface layers of different conductivity and susceptibility.

Kisabeth and Rostoker (1971) show that the fields associated with polar magnetic substorms are aperiodic and indicate that the structure of polar magnetic substorms is controlled by the intensification of



the currents at the northern and/or southern borders of the auroral electrojet. They propose that quasi-periodic intensifications of the northern border of the electrojet are responsible for the jagged structure noted on magnetograms during the substorms. It is therefore of interest to consider the effects at the surface of a finitely conducting earth due to multiple current system distributions.

Within the limitations of the two-dimensional problem, a double current system may be studied by an adaptation of the method of Peltier and Hermance (1971) and the results of section 4 for investigating non-uniform sources. The two current systems, which may be spatially displaced relative to one another and which may be made to vary aperiodically with time, can have maximum intensities which may occur at different times and so the current system as a whole will vary spatially.

In the present discussion the two current system distributions flow above an earth with a horizontally layered conductivity distribution. One system has a Gaussian current intensity distribution,  $\exp(-y^2/2k^2)$ . The other system has a current intensity distribution of  $y \cdot \exp(-ay)$ . Each system may vary aperiodically with time by summing the solutions for different frequencies through



the use of the Fourier transform. The spatially varying solution is obtained from the superposition of the separate aperiodic time solutions.

#### 5.1.b Method of Solution

The coordinate system is shown in Fig. 5.1. The Gaussian current source is symmetric about the origin (see Fig. 5.2) and the current flows parallel to the surface of the earth at a height of 110 km. In the following, this source will be referred to as the symmetric source. The second source, with current intensity distribution of the form  $y \cdot \exp(-ay)$  will be referred to as the non-symmetric source. The current associated with this latter source also flows parallel to the surface of the earth at a height of 110 km. The non-symmetric source has been displaced 700 km. in the positive  $y$  direction from the symmetric source (see Fig. 5.2). Values for the magnetic field components due to the two current systems are obtained at intervals of 100km. in the region  $-1000 \text{ km.} < y < 1000 \text{ km.}$

For the E-polarization case, certain symmetric and non-symmetric current distributions yield solutions for the two-dimensional diffusion equation which results

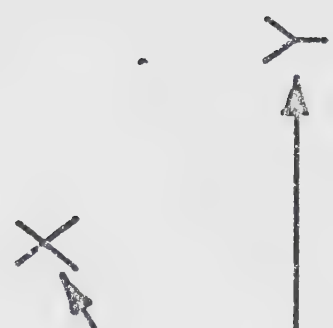
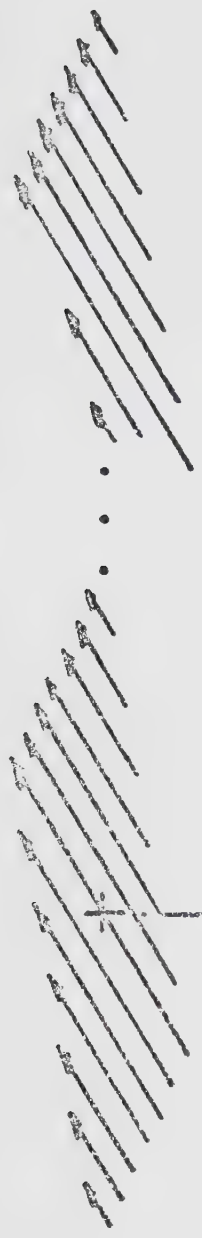






Fig. 5.1      The coordinate system, symmetric and non-symmetric source configuration and layered earth structure.

current  
source



1

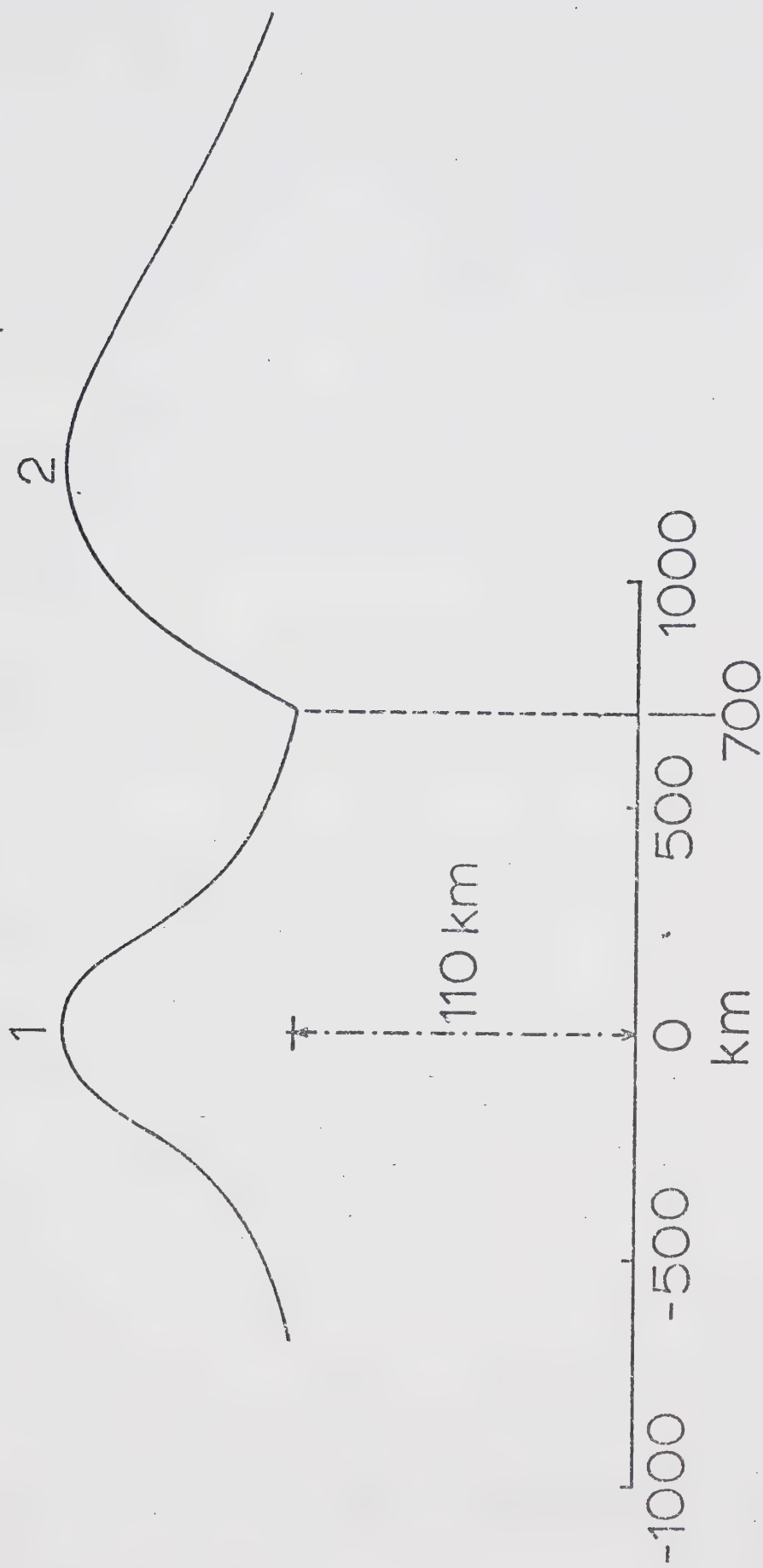
2

3





Fig. 5.2      Source position with respect to the region  
where magnetic field component values are  
calculated.







when the period is sufficiently long so that displacement currents may be neglected. In the E-polarization case (Jones and Price, 1970), this equation is the same as (1.9).

As shown in section 4 for a horizontally layered earth and for an inducing field with sinusoidal time dependence, the electric field in the nth layer can be written as

$$E_x^N(y,z) = \int_0^{\infty} \{A_n(P) \cdot \exp(-P \cdot z) + B_n(P) \cdot \exp(P \cdot z)\} \cdot \{V(s) \cdot \cos(sy) + W(s) \cdot \sin(sy)\} ds \quad (5.1)$$

where the constants  $A_n(P)$  and  $B_n(P)$  are defined by (4.4) through (4.9) and  $(P)^2 = s^2 + i\omega\mu \cdot V_n$ .

For a symmetric source over a two-layered earth it has been shown in section 4.1.a that

$$V(s) = -(iI \cdot \omega \mu k / \sqrt{2\pi} s) \cdot \exp(sz_0 - s^2 k^2 / 2) \quad (5.2)$$

and

$$W(s) = 0 \quad (5.3)$$

where  $I \cdot$  is the maximum current intensity, and  $k$  is the



standard deviation at the source. Referring to section 4.2.a, the non-symmetric current source distribution is

$$I_x(y^0) = I_0 \cdot (y^0 - b) \cdot \exp\{-a(y^0 - b)\} \cdot u(y^0 - b) \quad (5.4)$$

where  $b$  and  $a$  are constants,  $u(y^0 - b)$  is the unit step function, and

$$V(s) = -(i\omega I_0 \cdot \exp(sz^0) / 2\pi s) \cdot \{[(a^2 - s^2) \cdot \cos(sb) - 2as \cdot \sin(sb)] / (a^2 + b^2)^2\} \quad (5.5)$$

and

$$W(s) = -(i\omega I_0 \cdot \exp(sz^0) / 2\pi s) \cdot \{[2as \cdot \cos(sb) + (a^2 - s^2) \cdot \sin(sb)] / (a^2 + s^2)^2\}. \quad (5.6)$$

The magnetic field is obtained by taking the curl of (5.1) and the components are expressed as:

$$H_y^N(y, z) = -(i/\omega\mu) \cdot \int_0^\infty P \{A_n(P) \cdot \exp(-P \cdot z) - B_n(P) \cdot \exp(P \cdot z)\} \cdot \{V(s) \cdot \cos(sy) + W(s) \cdot \sin(sy)\} ds \quad (5.7)$$

and



$$H_z^N(y, z) = + (i/wu) \cdot \int_0^\infty s \{A_n(P) \cdot \exp(-P \cdot z) + B_n(P) \cdot \exp(P \cdot z)\} \cdot \{V(s) \cdot \sin(sy) - W(s) \cdot \cos(sy)\} ds. \quad (5.8)$$

The aperiodic solution is obtained for the magnetic field values by writing

$$H_y(y, t) = \int_{-\infty}^{\infty} H_y^1(y, w) \cdot F(w) \cdot \exp(iwt) dw, \quad (5.9)$$

and

$$H_z(y, t) = \int_{-\infty}^{\infty} H_z^1(y, w) \cdot F(w) \cdot \exp(iwt) dw \quad (5.10)$$

where  $F(w)$  is the Fourier transform of the time variation  $f(t)$  of the current source,

$$F(w) = (1/2\pi) \cdot \int_{-\infty}^{\infty} f(t) \cdot \exp(iwt) dt. \quad (5.11)$$

$H_y(y, t)$  and  $H_z(y, t)$  are the magnetic field responses as a function of time.

The two magnetic field components of both sources were calculated along the surface of a



horizontally layered earth with two layers. The upper layer has thickness 50 km. and resistivity of 100 ohm-m. The second layer is of infinite depth and resistivity 10 ohm-m.

The symmetric source has a current distribution

$$I = I_0 \cdot \exp(-y^2/2k^2), \quad (5.12)$$

where the half-width ( $k$ ) is 240 km. The non-symmetric source has a current distribution

$$I = I_0 \cdot (y-b) \cdot \exp(-a[y-b]) \cdot u(y-b) \quad (5.13)$$

where  $b=700$  km.,  $a=2.1 \times 10^{-4}$  km. $^{-1}$  and  $u$  is the unit step function. (Refer to Fig. 5.2 for relative source positions.)

The time variation of both current distributions is the same:

$$f(t) = \exp\{-d^2 \cdot (t-q)^2\}. \quad (5.14)$$

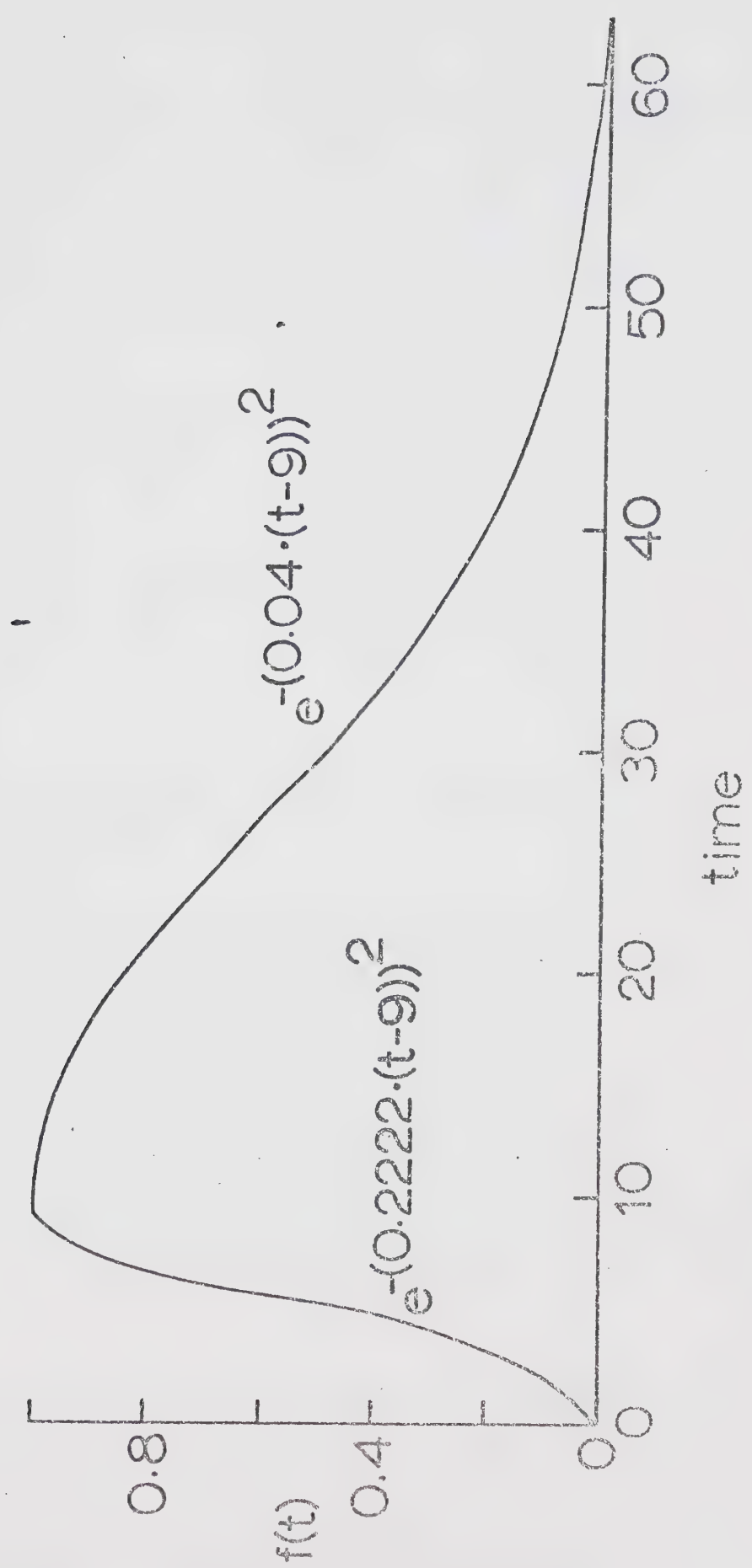
For  $0 < t < 9$  minutes  $d=0.2222$  and for  $9 < t < 63$  minutes  $d=0.040$ . The time variation is shown in Fig 5.3.







Fig. 5.3      Time variation of the current sources.





The Fourier spectrum of the current distribution time variation must be band limited to less than 1 Hz or the approximation that displacement currents may be neglected will not apply. The frequency spectrum of the time function chosen is negligible above 0.1 Hz.

The time variation of the magnetic field components  $H_y$  and  $H_z$  over the region of interest on the surface is shown in Fig. 5.4 for the symmetric source and Fig. 5.5 for the non-symmetric source. Starting with time  $t=0$  a total time span of 63 minutes is shown at time intervals of one minute.

#### 5.1.c The Two-Dimensional Aperiodic Spatially Varying Double Current Solution.

As outlined before, the aperiodic spatially varying source is obtained by the superposition of the symmetric and non-symmetric magnetic field component solutions. The non-symmetric source lags the symmetric source by ten minutes in time. The time variation for the composite source is shown in Fig. 5.6 with a time span of 74 minutes and time intervals the same as in Figs. 5.4 and 5.5.

The symmetric source, which is centered with







Fig. 5.4      The variation of  $H_y$  (below) and  $H_z$  (above)  
spatial profiles with time for the symmetric  
source.

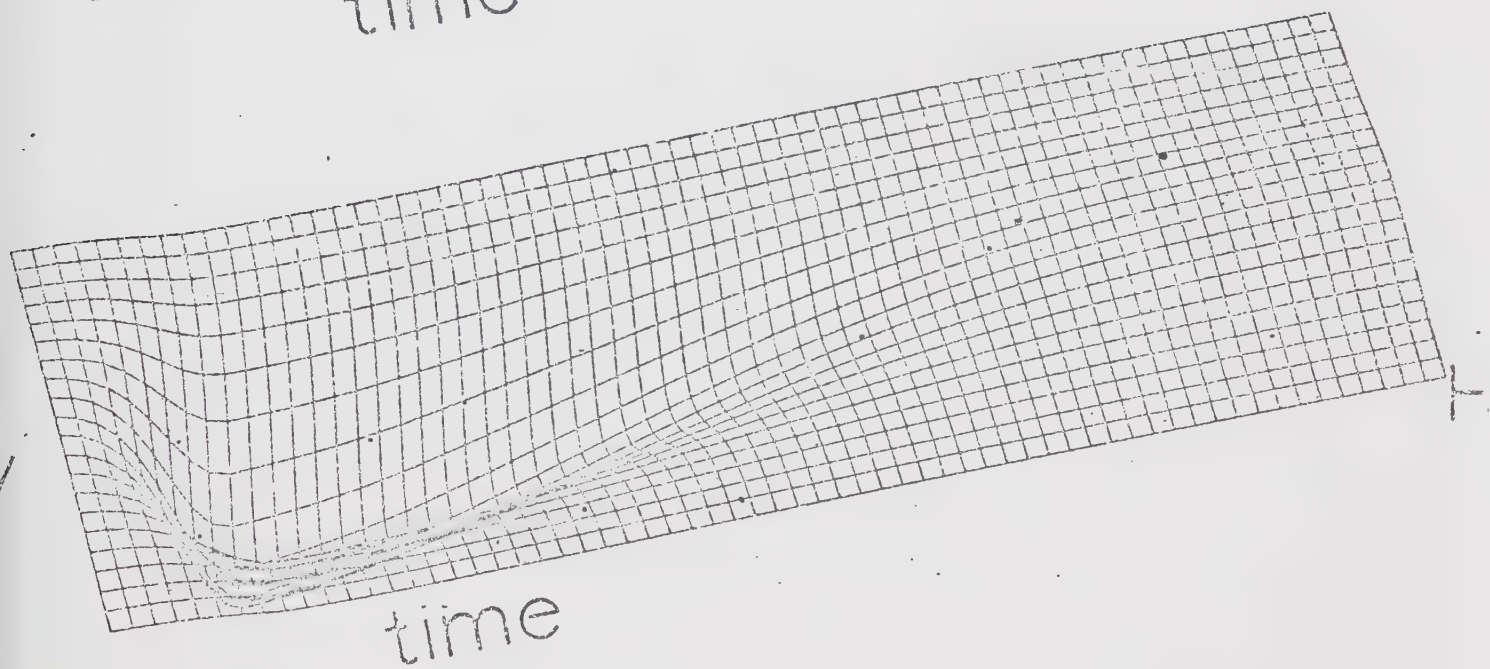
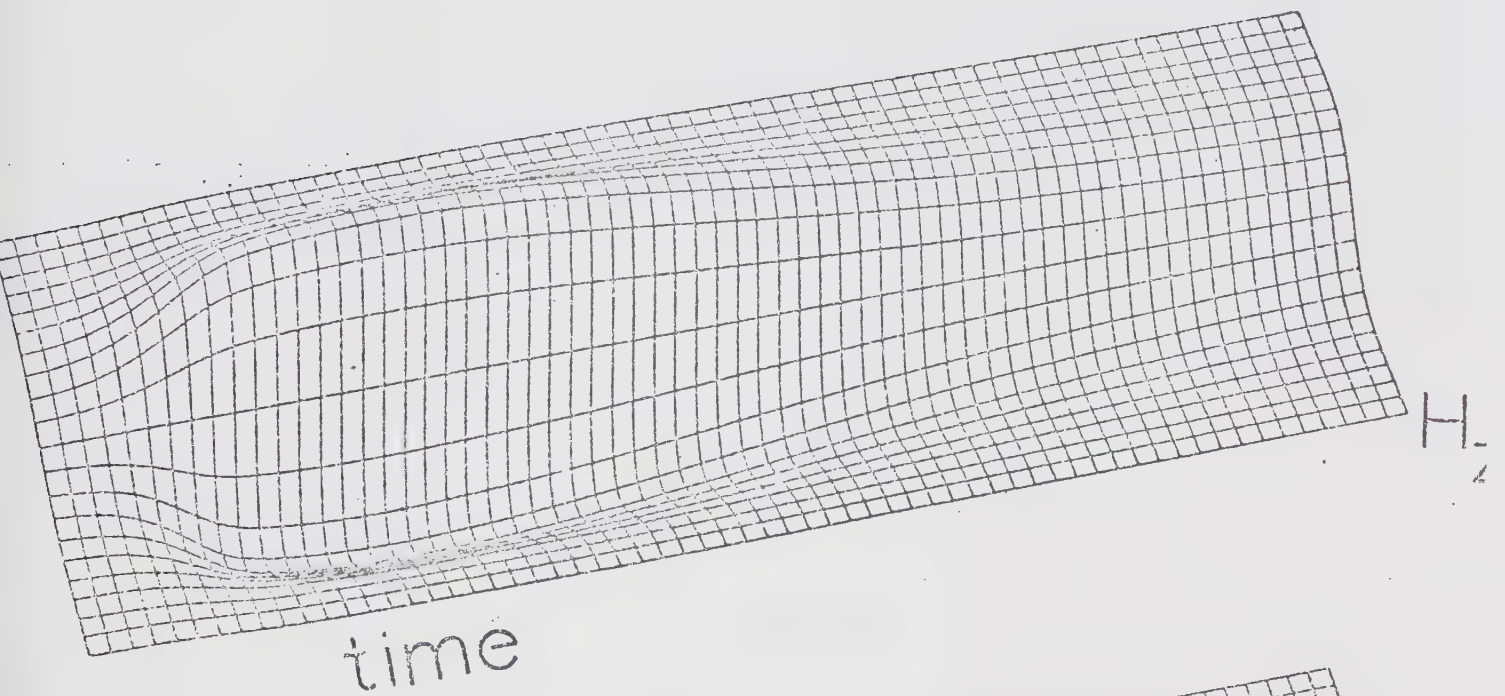






Fig. 5.5      The variation of  $H_y$  (below) and  $H_z$  (above)  
spatial profiles with time for the non-  
symmetric source.

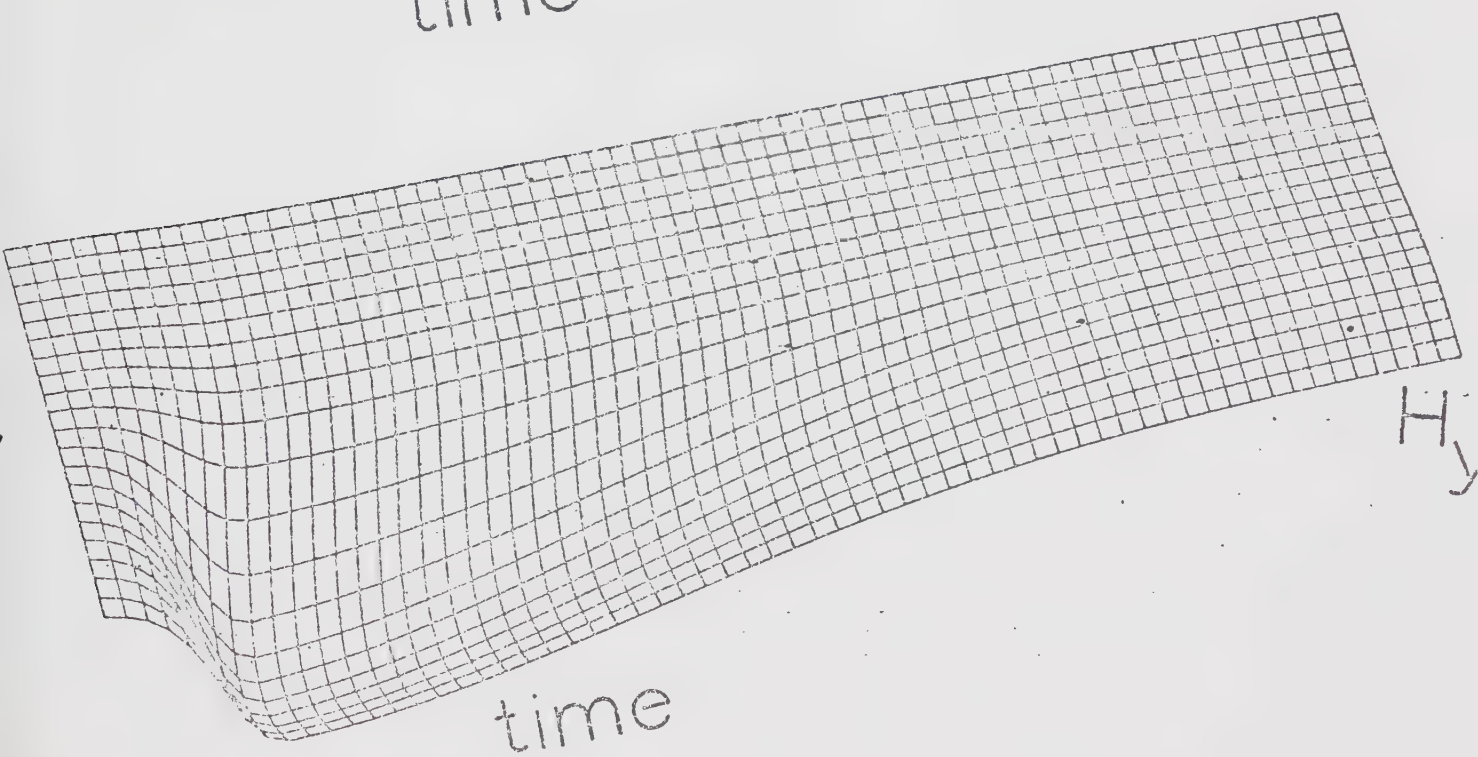
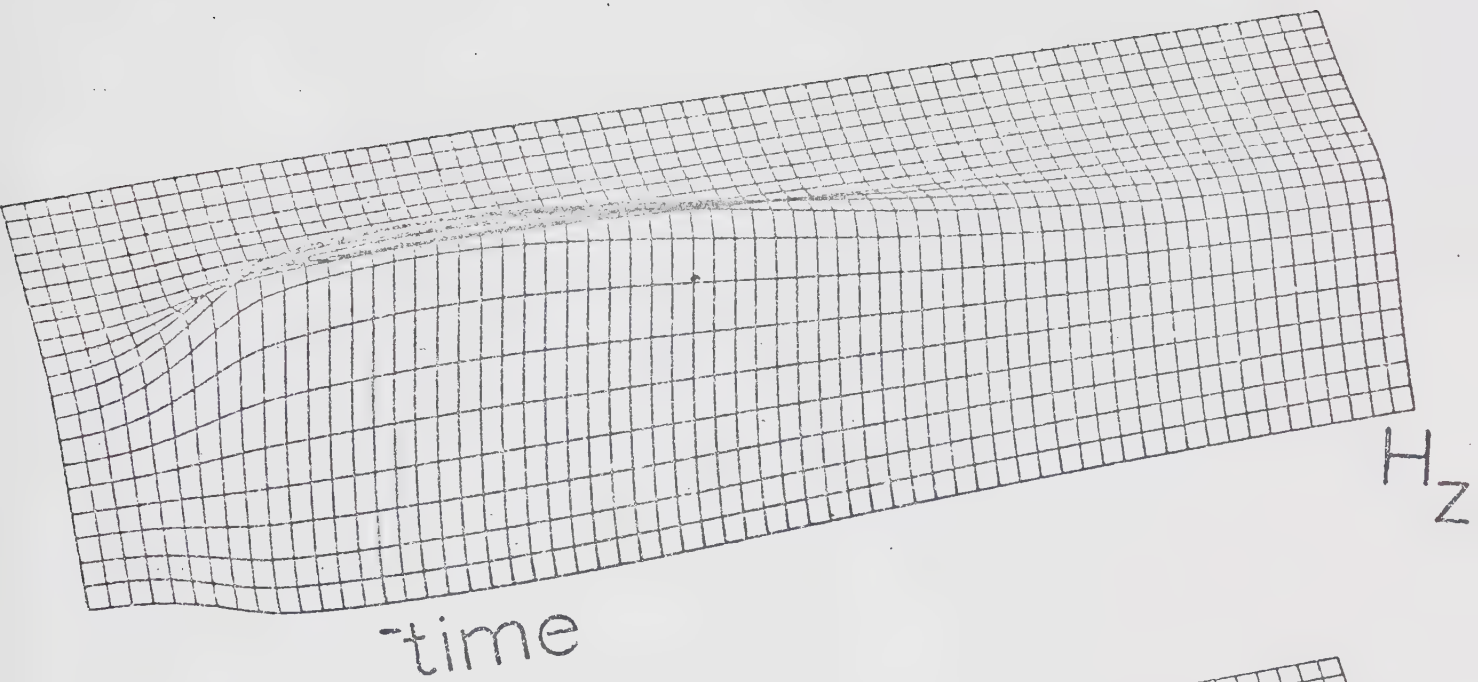
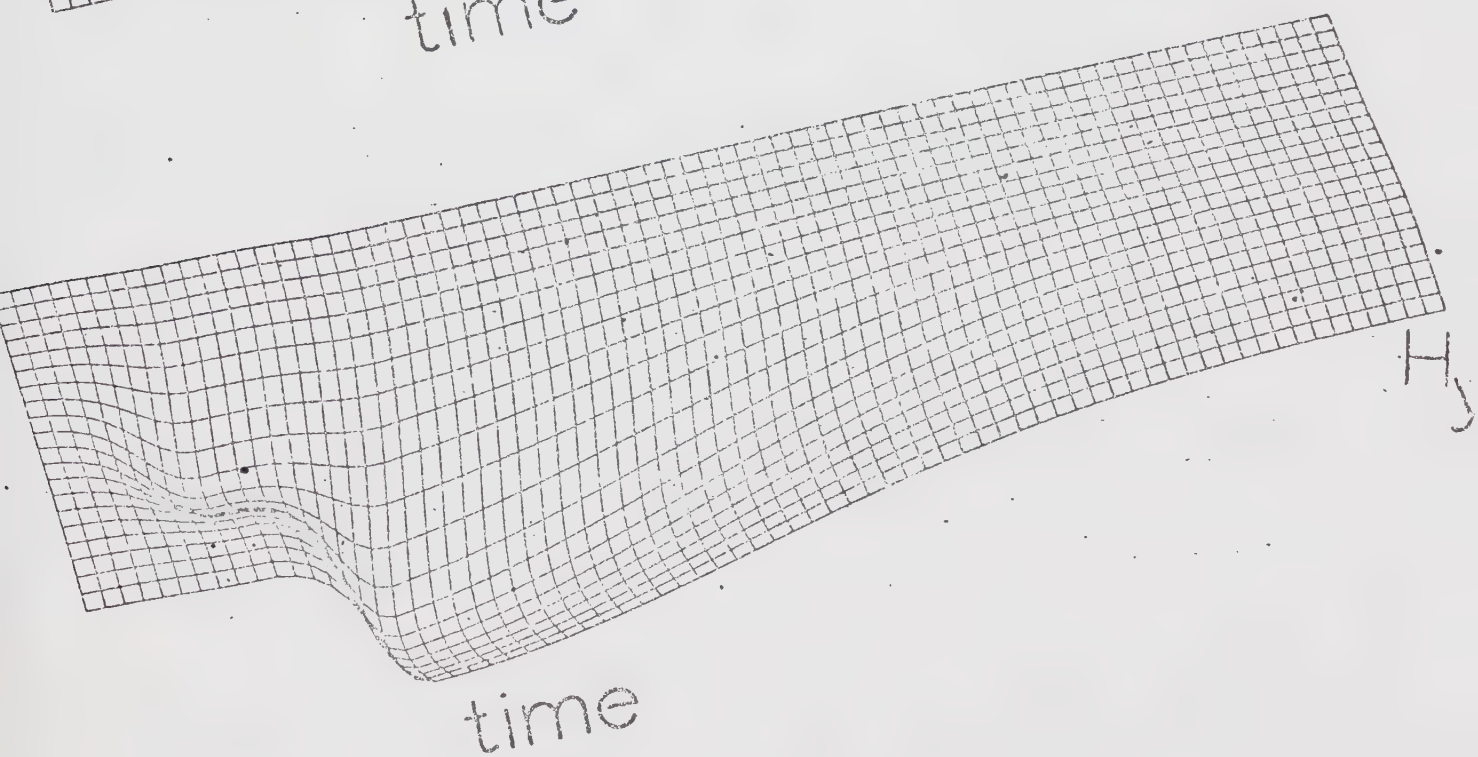
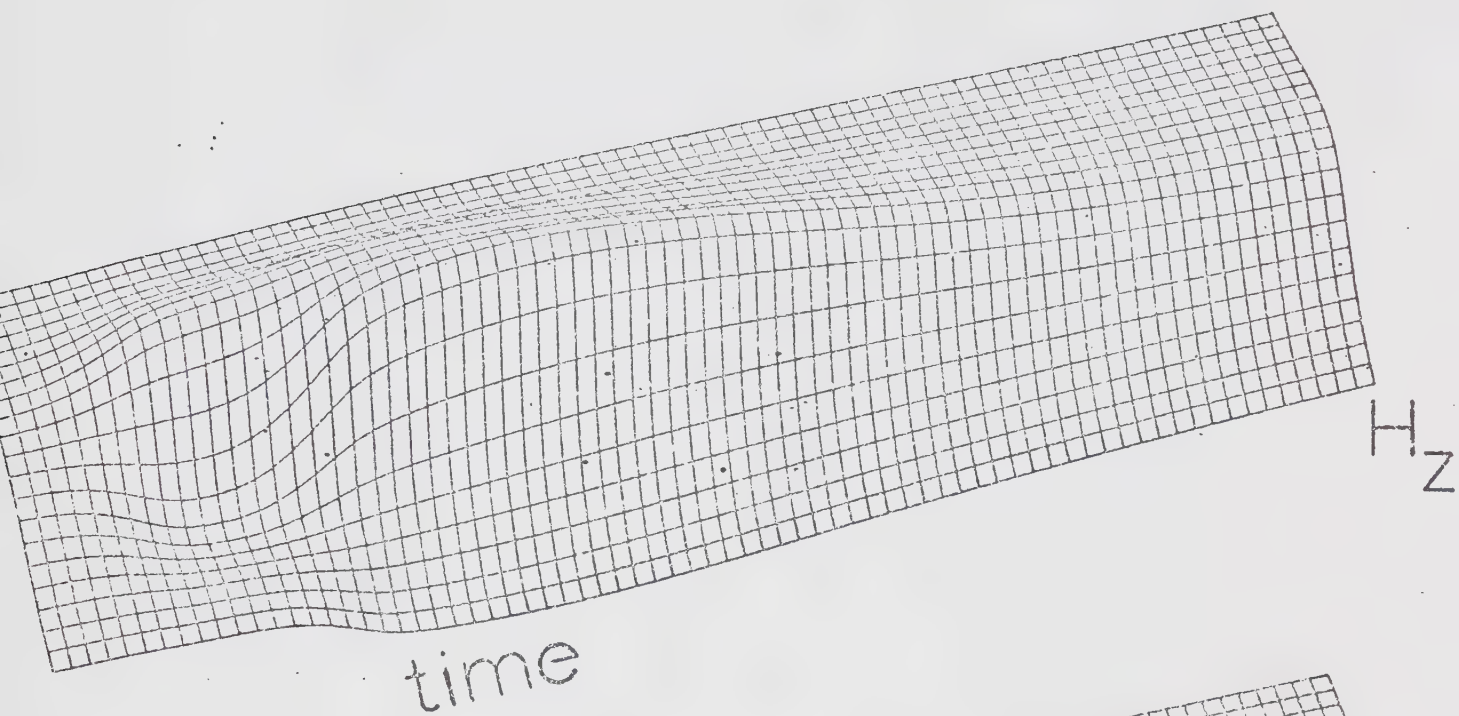








Fig. 5.6      The variation of  $H_y$  (below) and  $H_z$  (above) spatial profiles with time for the superimposed symmetric and non-symmetric source with the non-symmetric source lagging 10 minutes in time behind the symmetric source.





respect to the origin produces an  $H_y$  magnetic field component at the surface which is also symmetric about the origin. The  $H_z$  cross-over point (the point at which  $H_z$  equals zero) coincides with the origin as can be seen in Fig. 5.4. The non-symmetric source, having most of its current concentration positioned to the right of the region where the calculations of the magnetic field components were obtained, shows a high degree of non-symmetry in both the  $H_y$  and  $H_z$  magnetic field components as is evidenced in Fig. 5.5. The fact that the current concentration is to the right of the region of interest is clearly indicated by the position of the maximum value of  $H_y$  and the cross-over point of  $H_z$ . When the two sources are superimposed the magnetic field component configuration "moves" spatially with time.  $H_y$  exhibits two maxima in time at different positions along the surface as can be seen in Fig. 5.6. The cross-over point of  $H_z$  shifts to the right with time as can be seen in Figs. 5.7, 5.8 and 5.9. These are spatial profiles of the  $H_y$  and  $H_z$  components for intervals of time four minutes apart starting at  $t=0$ .

The non-symmetry in the surface profile of the  $H_y$  component (Fig. 5.7) for the first two time intervals is due to the fact that the contribution of the non-





Fig. 5.7      Spatial profiles of  $H_y$  and  $H_z$  where the magnetic field values have been normalized with respect to the field component values at the origin at  $t=0$ .

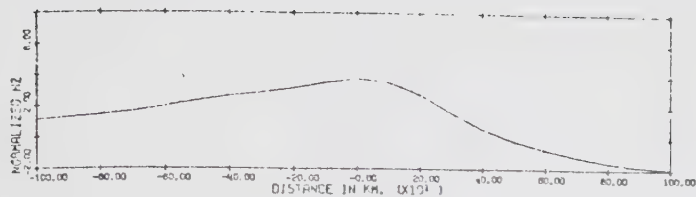




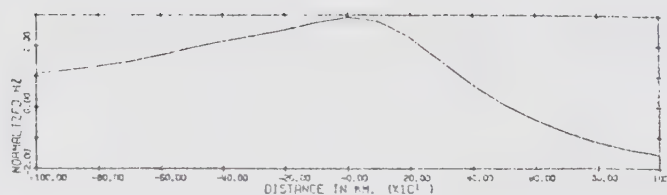




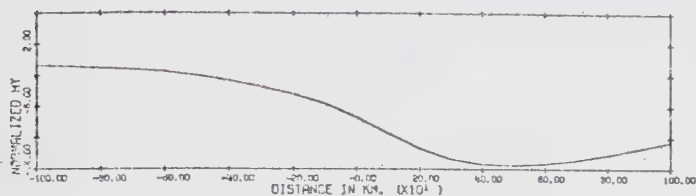
Fig. 5.8      Spatial profiles of  $H_y$  and  $H_z$  where the magnetic field values have been normalized with respect to the field component values at the origin at  $t=0$ .



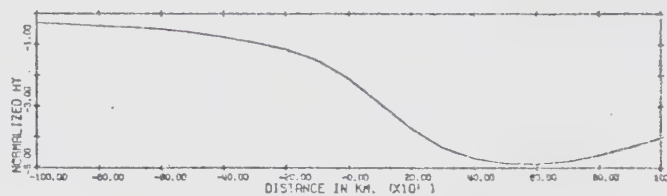
PROFILE OF HZ VERSUS DISTANCE T=31 MINUTES



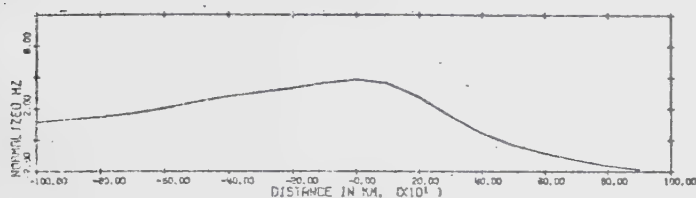
PROFILE OF HZ VERSUS DISTANCE T=43 MINUTES



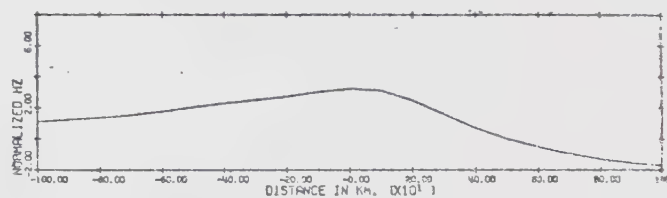
PROFILE OF HY VERSUS DISTANCE T=31 MINUTES



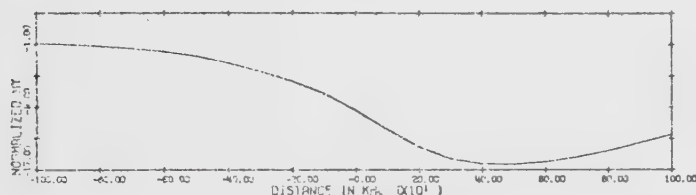
PROFILE OF HY VERSUS DISTANCE T=43 MINUTES



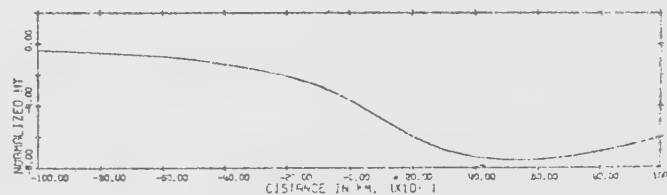
PROFILE OF HZ VERSUS DISTANCE T=27 MINUTES



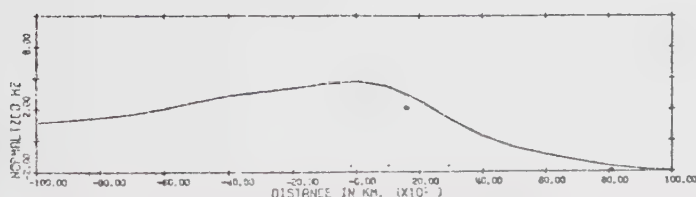
PROFILE OF HZ VERSUS DISTANCE T=39 MINUTES



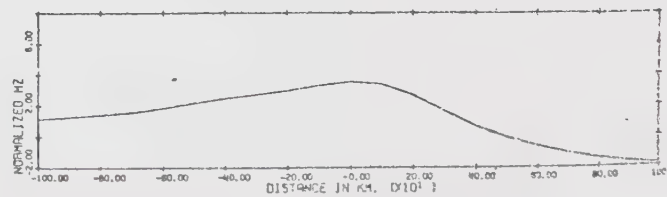
PROFILE OF HY VERSUS DISTANCE T=27 MINUTES



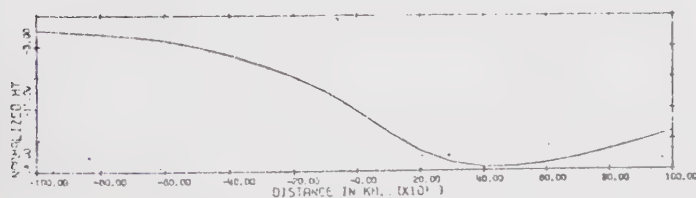
PROFILE OF HY VERSUS DISTANCE T=39 MINUTES



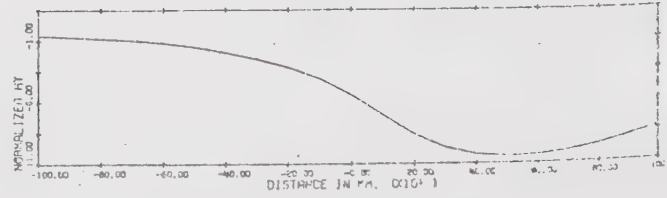
PROFILE OF HZ VERSUS DISTANCE T=23 MINUTES



PROFILE OF HZ VERSUS DISTANCE T=35 MINUTES



PROFILE OF HY VERSUS DISTANCE T=23 MINUTES

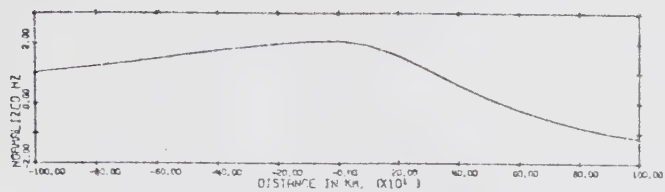


PROFILE OF HY VERSUS DISTANCE T=35 MINUTES

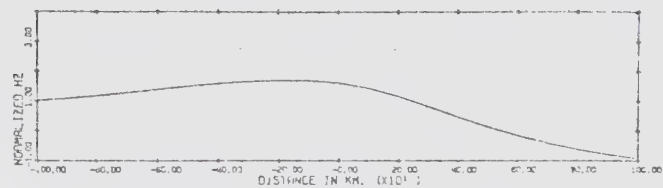




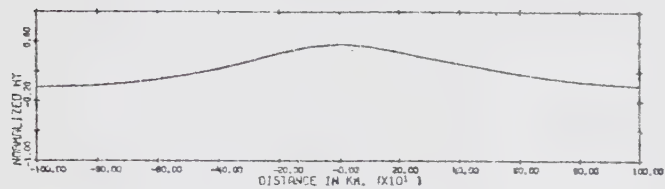
Fig. 5.9      Spatial profiles of  $H_y$  and  $H_z$  where the magnetic field values have been normalized with respect to the field component values at the origin at  $t=0$ .



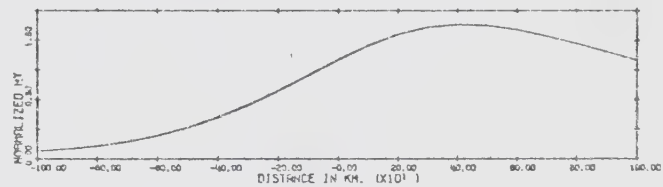
PROFILE OF HZ VERSUS DISTANCE T=55 MINUTES



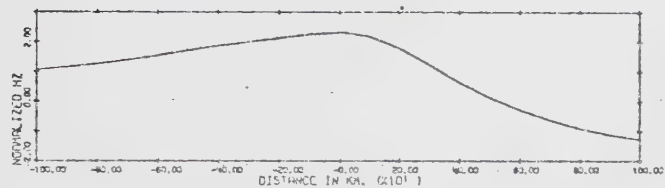
PROFILE OF HZ VERSUS DISTANCE T=67 MINUTES



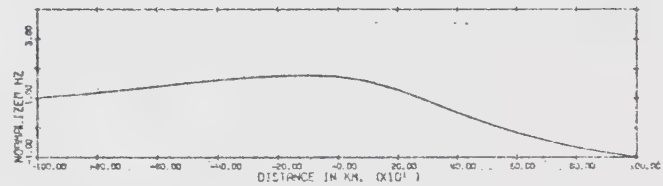
PROFILE OF HY VERSUS DISTANCE T=55 MINUTES



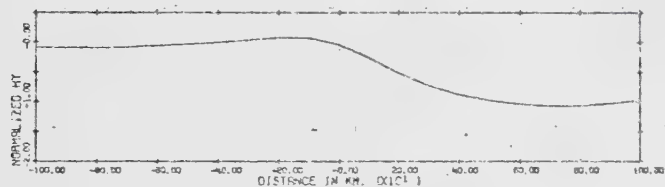
PROFILE OF HY VERSUS DISTANCE T=67 MINUTES



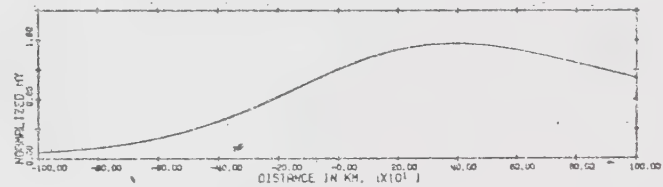
PROFILE OF HZ VERSUS DISTANCE T=81 MINUTES



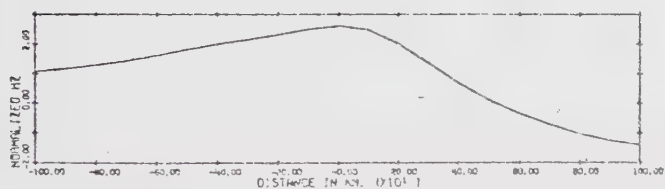
PROFILE OF HZ VERSUS DISTANCE T=63 MINUTES



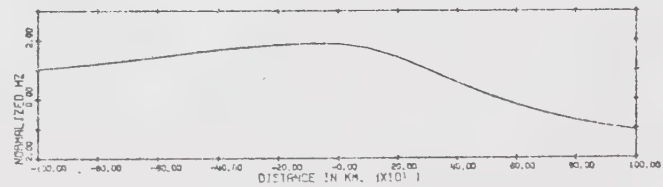
PROFILE OF HY VERSUS DISTANCE T=51 MINUTES



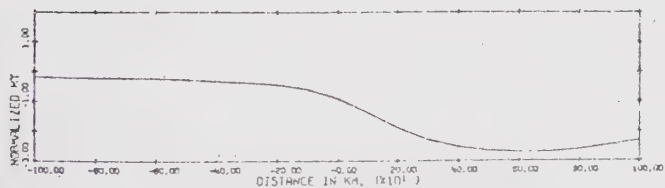
PROFILE OF HY VERSUS DISTANCE T=63 MINUTES



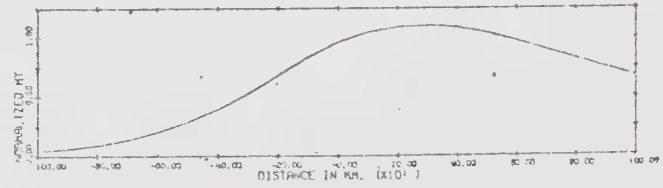
PROFILE OF HZ VERSUS DISTANCE T=47 MINUTES



PROFILE OF HZ VERSUS DISTANCE T=53 MINUTES



PROFILE OF HY VERSUS DISTANCE T=47 MINUTES



PROFILE OF HY VERSUS DISTANCE T=59 MINUTES





symmetric source was held constant for the first 10 minutes. The initial values of  $H_y$  at  $t=0$  of Fig 5.5 were used for the non-symmetric source contribution of Fig. 5.6 for  $t=0$  minutes through  $t=10$  minutes. In Fig. 5.6 for  $t \geq 63$  minutes, the symmetric source was held constant at its final value ( $t=63$  minutes, Fig. 5.4). The same procedure was followed for the calculation of the  $H_z$  component in Fig. 5.6, 5.7, 5.8 and 5.9.

Kisabeth and Rostoker (1971) and Kisabeth (1972) have observed a latitudinal movement of the  $H_z$  cross-over associated with polar magnetic substorms, and it is apparent that this work supports their conclusions with reference to the double current sources.



## 6. RECOMMENDATIONS FOR FURTHER RESEARCH

The three-dimensionality of the physical electromagnetic induction problem causes difficulty if the direct application of the previously discussed methods of sections 4 and 5 to actual observed data is attempted. As pointed out by Onwumechilli (1967) allowance must be made for return currents, such that the forward current equals the return current. This can be accomplished by combining several symmetric and non-symmetric sources such that magnetic field profiles fit the observed data.

(e.g. One symmetric source can be allowed to flow parallel to the x axis with two non-symmetric sources, one at either side, flowing antiparallel.) If two aperiodic sources which allow for return currents are then superimposed as in section 5, it should be possible to make the spatial shift of the magnetic field components fit the actual observations.



## REFERENCES

- Ashour, A.A., 1950. The induction of electric currents in a uniform circular disk.  
Quart. J. Mech. Appl. Math., 3, 119-127.
- Cagniard, L., 1953. Basic theory of the magneto-telluric method of geophysical prospecting.  
Geophysics 18, 605-635.
- Chapman, S., 1919. The solar and lunar diurnal variations of terrestrial magnetism.  
Phil. Trans. Roy. Soc. London, A, 218, 1-118.
- Chapman, S., and Price, A.T., 1930. The electric and magnetic state of the interior of the earth as inferred from terrestrial magnetic variations. Phil. Trans. Roy. Soc. London, A, 229, 427-460.
- Chapman, S., and Whitehead, T.T., 1922. The influence of electrically conducting material within the earth on various phenomena of terrestrial magnetism. Trans. Phil. Soc. Cambridge 22, 463-482.
- Coggon, J.H., 1971. Electromagnetic and electrical modeling by the finite element method.



Geophysics 36, 132-155.

D'Erceville, I., and Kunetz, G., 1962. The effect of a fault on the earth's natural electromagnetic field. Geophysics 27, 651-665.

Dosso, H.W., and Jacobs, J.A., 1968. Analogue model measurements of electromagnetic variations in the near field of an oscillating line current. Can. J. Earth Sci. 5, 23-29.

Dulaney, E.N., and Madden, T.R., 1962. Analogue relaxation net calculation of two-dimensional magnetotelluric response curves. S.E.G. Yearbook, p. 265 (Abstract).

Erdelyi, A., Magnus, W., Oberhettinger, F. and Tricomi, F., 1954. Tables of Integral Transforms. 1, McGraw-Hill Book Co. Inc. New York.

Forbush, S.E., and Casaverde, M., 1961. The equatorial electrojet in Peru. Carnegie Inst. Wash. Publ. 620.

Hermance, J.F., and Peltier, W.R., 1970. Magnetotelluric fields of a line current. J. Geophys. Res. 75, 3351-3356.

Hibbs, R.D., and Jones, F.W., 1972a. Apparent resistivity calculations for laterally inhomogeneous structures. Phys. Earth Planet. Int. 5, 184-189.





- Hibbs, R.D., and Jones, F.W., 1972b. Electromagnetic induction in the earth by a symmetric non-uniform source. Geophys. J. R. astr. Soc. Submitted.
- Hibbs, R.D., and Jones, F.W., 1972c. Electromagnetic induction in the earth by a non-symmetric non-uniform source. In preparation.
- Jones, F.W., 1971a. Electromagnetic induction in a non-horizontally stratified two-layered conductor. Geophys. J. R. astr. Soc. 22, 17-28.
- Jones, F.W., 1971b. Electromagnetic induction in a two-dimensional model of an asymmetric two-layered conductor. Phys. Earth Planet. Interiors 4, 417-424.
- Jones, F.W., and Pascoe, L.J., 1971. A general computer program to determine the perturbation of alternating electric currents in a two-dimensional model of a region of uniform conductivity with an embedded inhomogeneity. Geophys. J.R. astr. Soc. 24, 3-30.
- Jones, F.W., and Price, A.T., 1969. The perturbation of an alternating field by a conductivity anomaly. I.A.G.A. Bulletin 26 (Abstract



III-106) p. 196.

Jones, F.W., and Price, A.T., 1970. The perturbations of alternating geomagnetic fields by conductivity anomalies.

Geophys. J. R. astr. Soc. 20, 317-334.

Jones, F.W., and Price, A.T., 1971a. The geomagnetic effects of two-dimensional conductivity inhomogeneities at different depths.

Geophys. J. R. astr. Soc. 22, 333-345.

Jones, F.W., and Price, A.T., 1971b. Geomagnetic effects of sloping and shelving discontinuities of earth conductivity. Geophysics 36, 58-66.

Kisabeth, J.L., 1972. The dynamical development of the polar electrojets. Ph.D. Thesis. Univ. of Alberta.

Kisabeth, J.L. and Rostoker, G., 1971. Development of the polar electrojet during polar magnetic substorms. J. Geophys. Res. 76, 6815-6828.

Lahiri, B.N., and Price, A.T., 1939. Electromagnetic induction in non-uniform conductors, and the determination of the conductivity of the earth from terrestrial magnetic variations. Phil. Trans. Roy. Soc. London, A, 237, 509-540.

Lamb, H., 1883. On electrical motions in a spherical



conductor. Phil. Trans. Roy. Soc. London A,  
174, 519-549.

Latka, R., 1966. Modellrechnungen zur Induktion im  
elektrisch leitfähigen untergrund.  
Zeitschrift für Geophysik 32, 512-517.

Madden, T., and Thompson, W., 1965. Low frequency  
electromagnetic oscillations of the earth-  
ionosphere cavity. Rev. Geophys. 3, 211-  
254.

Madden, T.R., and Swift, C.M., 1969. Magnetotelluric  
studies of the electrical conductivity  
structure of the crust and upper mantle. In  
The Earth's Crust and Upper Mantle, edited  
by P.J. Hart, pp. 469-479. A.G.U.  
Monograph 13.

Mann, J.E., 1970. A perturbation technique for solving  
boundary value problems arising in the  
electrodynamics of conducting bodies.  
Appl. Sci. Res. 22, 113-126.

Neves, A., 1957. The generalized magneto-telluric method.  
Ph.D. thesis. Dept. of Geol. and Geophys.,  
M.I.T.

Onwumechelli, A., 1967. Geomagnetic variations in the  
equatorial zone. Physics of Geomagnetic



Phenomena (eds. S. Matsushita and  
W.H. Campbell), 1, p. 425.

Pascoe, L.J., and Jones, F.W., 1972. Boundary conditions  
and calculation of surface values for the  
general two-dimensional electromagnetic  
induction problem.

Geophys. J. R. astr. Soc. 27, 179-193.

Patrick, F.W., and Bostick, F.X., 1969. Magnetotelluric  
modelling techniques. Tech. Rept. 59.  
Electronics Research Center, Univ. of Texas,  
Austin.

Peltier, W.R., and Hermance, J.F., 1971. Magnetotelluric  
fields of a Gaussian electrojet.  
Can. J. Earth Sci. 8, 338-346.

Price, A.T., 1930. Electromagnetic induction in a  
conducting sphere. Proc. London Math. Soc.,  
(2), 31, 217-224.

Price, A.T., 1931. Electromagnetic induction in a  
permeable conducting sphere. Proc. London  
Math. Soc. (2), 33, 233-245.

Price, A.T., 1949. The induction of electric currents in  
non-uniform thin sheets and shells.  
Quart. J. Mech. Appl. Math. 2, 283-310.

Price, A.T., 1950. Electromagnetic induction in a semi-  
infinite conductor with a plane boundary.





- Quart. J. Mech. Appl. Math. 3, 385-410.
- Price, A.T., 1962. The theory of magnetotelluric fields when the source field is considered. J. Geophys. Res. 67, 1907-1918.
- Price, A.T., 1964. A note on the interpretation of magnetic variations and magnetotelluric data. J. Geomagn. Geoelect. 15, 241-248.
- Price, A.T., 1965. Effects of induced earth currents on low-frequency electromagnetic oscillations. Radio Science J. Res. NBS/USNC-URSI 69D (8), 1161-1168.
- Rankin, D., 1962. The magneto-telluric effect on a dike. Geophysics 27, 666-676.
- Reddy, I.K., and Rankin, D., 1972. Magnetotelluric response of a two-dimensional sloping contact by the finite element method. Submitted.
- Rikitake, T., 1950. Electromagnetic induction within the earth and its relation to the electrical state of the earth's interior. Bull. Earthquake Res. Inst. Tokyo Univ., 28, 45-100 and 219-283.
- Rikitake, T., 1960. Electromagnetic induction in a hemispherical ocean by Sq.



- J. Geomagn. Geoelect. 11, 65-79.
- Rikitake, T., 1961. Sq and Ocean. J. Geophys. Res. 66, 3245.
- Rikitake, T., 1966. Electromagnetism and the Earth's Interior, Elsevier Publishing Company.
- Ryu, J., 1972. Finite element method to electromagnetic induction problems in geophysics. Trans. A. G. U. 53, p. 361. Abstract GP58.
- Schmucker, U., 1971. Electromagnetic induction in a non-uniform layer of finite thickness. XV IUGG General Assembly, Moscow, Abstract III-19, p. 300.
- Schuster, A., 1889. The diurnal variation of terrestrial magnetism. Phil. Trans. Roy. Soc. London, A, 208, 163-204.
- Smith, G.D., 1969. Numerical Solution of Partial Differential Equations. Oxford Univ. Press.
- Swift, C.M., 1967. A magnetotelluric investigation of an electrical conductivity anomaly in the Southwestern United States. Ph.D. thesis, Dept. of Geol. and Geophys., M.I.T.
- Swift, C.M., 1971. Theoretical magnetotelluric and terrain response from two-dimensional inhomogeneities. Geophysics 36, 38-52.



- Tranter, C.J., 1965. Integral Transforms in Mathematical Physics. Methuen, London.
- Wait, J.R., 1954. On the relation between telluric currents and the earth's magnetic field. Geophysics 19, 281-289.
- Wait, J.R., 1962. Electromagnetic Waves in Stratified Media. Pergamon Press.
- Ward, S.H., and Morrison, H.F., 1966. Discussion of a paper by Hoffman and Horton. J. Geophys. Res. 71, 4053-4054.
- Weaver, J.T., 1963. The electromagnetic field within a discontinuous conductor with reference to geomagnetic micropulsations near a coastline. Can. J. Phys. 41, 484-495.
- Weaver, J.T., and Thomson, D.J., 1972. Induction in a non-uniform conducting half-space by an external line current. Geophys. J.R. astr. Soc. 28, 163-185.
- Wright, J.A., 1969. The magnetotelluric and geomagnetic response of two-dimensional structures. GAMMA (Inst. Geophysik Meteorologie Tech. Univ. Braunschweig) 1, 102S.
- Wright, J.A., 1970. Anisotropic apparent resistivities arising from non-homogeneous two-dimensional



structures. Can. J. Earth Sci. 1, 527-531.

















**B30028**